Applied Energy 335 (2023) 120752

Contents lists available at ScienceDirect

Applied Energy

journal homepage: www.elsevier.com/locate/apenergy

Efficient energy storage in residential buildings integrated with RESHeat system

Mehmet Ali Yildirim [a,*], Filip Bartyzel [a], Andrea Vallati [b], Magdalena Kozień Woźniak [c], Paweł Ocłoń [a,*]

[a] Department of Energy, Cracow University of Technology, ul. Warszawska 24, 31-155, Cracow, Poland
[b] Department of Astronautical, Electrical and Energy Engineering, Sapienza University of Rome, Via Eudossiana 18, 00184, Rome, Italy
[c] Faculty of Architecture, Cracow University of Technology, ul. Warszawska 24, 31-155, Cracow, Poland

HIGHLIGHTS

- A new renewable energy based heating system for buildings is presented.
- A mathematical model of the systems is developed using a TRNSYS software.
- System components models are validated with experimental data.
- The system covers 100% of building heating demand.
- The yearly average COP higher than 4.8 is achieved.

ARTICLE INFO

Keywords:
Energy storage
Thermal energy
photovoltaic-thermal systems (PV/T)
Solar energy
Underground thermal storage
NZEB residential buildings

ABSTRACT

The Renewable Energy System for Residential Building Heating and Electricity Production (RESHeat) system has been realized for heating and cooling residential buildings. The main components of the RESHeat system are a heat pump, photovoltaic modules, sun-tracking solar collectors and photovoltaic/thermal modules, an underground thermal energy storage unit, and a ground heat exchanger. One of the main novelties of the RESHeat system is efficient ground regeneration due to the underground energy storage unit. During a heating season, a large amount of heat is taken from the ground. The underground energy storage unit allows the restoration of ground heating capability and the heat pump's coefficient of performance (COP) to be kept high as possible for consecutive years. The paper presents an energy analysis for a residential building that is a RESHeat system demo site, along with integrating the RESHeat system with the building. The experimentally validated components coupled with the building model to achieve the system performance in TRNSYS software. The results show that the yearly average COP of the heat pump is 4.85 due to the underground energy storage unit. The RESHeat system is able to fully cover the heating demand of the building using renewable energy sources and an efficient underground energy storage system.

1. Introduction

The rise in energy prices and the desire to reduce the environmental impact of pollution emitted into the atmosphere encourage researchers and scientists to find solutions to cover the energy demand of residential buildings. The share of renewable energy in energy generation was still low as 22.1 % in 2020 by the European Union (EU). The use of renewable energy has many potential benefits, including a reduction in greenhouse gas emissions, the diversification of energy supplies, and a reduced dependency on fossil fuel markets. EU directives require the member states to increase the share of Renewable Energy Sources in the total energy mix – Directive 2009/28/EC, with a new emission reduction target of 50 % by 2030 compared with 2021.

Buildings are essential for the European Union's energy efficiency policy, as they account for 40 % of total energy consumption. In accordance with Directive 2010/31/EU of the European Parliament and of the Council [1] of 19 May 2010 on the energy performance of buildings, by 31 December 2020, all new buildings should be zero-energy buildings. The nearly zero or very low amount of energy

* Corresponding authors.
E-mail addresses: mehmet.yildirim@doktorant.pk.edu.pl (M. Ali Yildirim), pawel.oclon@pk.edu.pl (P. Ocłoń).

https://doi.org/10.1016/j.apenergy.2023.120752
Received 2 November 2022; Received in revised form 30 December 2022; Accepted 22 January 2023
Available online 2 February 2023
0306-2619/

Nomenclature

Abbreviations and acronyms

RESHeat	Renewable Energy System for Residential Building Heating and Electricity Production
COP	Coefficient of performance
NZEB	Nearly zero-energy building
PE	Primary Energy
GUS	Central Statistical Office
PV	Photovoltaic
STC	Standard test conditions
GW	Green wall
HVAC	Heating, ventilation, air conditioning
SAHP	Solar-assisted heat pump system
PCM	Phase-change material
SCADA	Supervisory control and data acquisition
PV/T	Photovoltaic/thermal system
SAGSHP	Solar-assisted ground heat pump systems
GSHP	Ground-source heat pump
GHG	Greenhouse gases
LCC	Life cycle cost
CCHP	Combined cooling, heating, and power
TMY	Typical meteorological year
CH	Central heating
DHW	Domestic hot water
SC	Solar collector
NOCT	Normal operating cell temperature
B2G	Borehole to ground
NPV	Net present value

Symbols

U	heat transfer coefficient, W/(m^2 × K)
$\dot{v}_{inf}$	infiltration rate, m^3/s
q_{air}	density of the air at a mean temperature, kg/m^3
c_p	the specific heat capacity of air at constant pressure, kJ/(kg × K)
T_{in}	air temperature inside the apartment, °C
T_{out}	ambient air temperature, °C
I_{SC}	short circuit current, A
V_{OC}	open-circuit voltage, V
I_{MPP}	current at maximum power point, A
V_{MPP}	Voltage at maximum power point, V
T_{real_out}	solar collector's actual outlet temperature, °C
T_{sim_out}	solar collector's simulation outlet temperature, °C
Q_{real_out}	actual thermal energy production of the solar collector, kW
Q_{sim_out}	simulation thermal energy production of the solar collector, kW
Q_{real}	actual thermal energy generation of PV/T system, W
Q_{sim}	simulation thermal energy generation of PV/T system, W
P_{real}	actual electricity generation of PV/T system, W
P_{sim}	simulation electricity generation of PV/T system, W
$T_{realtank\_lo}$	actual temperature at the bottom of the tank, °C
$T_{realtank\_top}$	actual temperature at the top of the tank, °C
$T_{simtank\_lo}$	simulation temperature at the bottom of the tank, °C
$T_{simtank\_top}$	simulation temperature at the top of the tank, °C
Q_{Total}	total energy demand of the storey, including CH, DHW, and losses, MWh/y
P_{hp}	electricity consumption of the heat pump, MWh/y
Q_{solar}	thermal energy generation of solar collectors, MWh/y
Q_{pvt}	thermal energy generation of PV/T system, MWh/y
$P_{pv\text{-}pvt}$	total electricity generation of the PV and PV/T systems, MWh/y
Q_{ch}	thermal energy demand for central heating, MWh/y
Q_{dhw}	thermal energy demand for domestic hot water preparation, MWh/y
T_{top}	top side temperature of the underground storage tank, °C
T_{lo}	bottom side temperature of the underground storage tank, °C
T_{av_us}	the mean temperature of the underground storage tank, °C
T_{amt}	ambient temperature, °C
T_{av_hx}	average borehole heat exchanger temperature, °C
T_{av_soil}	average soil temperature, °C
T_{in_PVT}	inlet temperature of PV/T system, °C
T_{out_PVT}	outlet temperature of the PV/T system, °C

required should be covered to a very significant extent by energy from renewable sources, including energy from renewable sources produced on-site or nearby, taking into account the following:

a) Decentralized energy supply systems based on energy from renewable sources.
b) Simultaneous generation in one process of thermal energy and electrical and/or mechanical energy.
c) District or block heating or cooling, particularly where it is based entirely or partially on energy from renewable sources.
d) Heat pumps.

In 2016, European Commission [2] made the recommendation 2016/1318 on guidelines for the promotion of nearly zero-energy buildings and best practices to ensure that, by 2020, all new buildings are nearly zero-energy buildings. The document explains the definition of such a building included in the EU Directive 2010/31. The concept of the nearly zero-energy building (NZEB) reflects the fact that renewable energy and efficiency measures work together. When placed on-building, renewable energy will reduce net delivered energy. In many cases, on-site renewable energy will not be sufficient to bring energy needs close to zero without further energy efficiency measures or a significant decrease in primary energy factors for off-site renewable energy sources. Therefore, higher and more demanding requirements for highly efficient NZEB will also drive increased use of on-building renewables, resulting in the adaptation of primary energy factors for off-site energy carriers, taking their renewable energy content into account. While the Directive sets the framework definition of NZEBs, its detailed application in practice (e.g., what is a 'very high energy performance' and what would be the recommended significant contribution of 'energy from renewable sources) is the responsibility of the Member States when they transpose Article 9 of the Directive into their national legal systems. The framework definition of NZEB in the Directive does not differentiate between new and existing buildings. 'Refurbishment into NZEB,' therefore, means a refurbishment of a magnitude that allows the energy performance requirements of an NZEB level to be met. This does not prevent having different timelines and financial support for existing buildings in recognition of the longer period required for NZEB levels to be cost-optimal in the case of existing buildings. In its recommendations, the European Commission draws attention to the fact that there cannot be a single level of ambition for NZEB across the EU. Flexibility is needed to account for the impact of climatic conditions on heating and cooling needs and on the cost-effectiveness of packages of energy efficiency and renewable energy sources measures. The index of annual demand for non-renewable primary energy (PE) determines the amount of energy required for heating, ventilation, domestic hot water preparation, cooling, and lighting. It depends on the type of building. For residential buildings, most Member States aim to have a primary energy use not higher than 50 kWh/(m^2 y). The maximal primary energy use ranges between 20 kWh/(m^2 y) in Denmark or 33 kWh/(m^2 y) in Croatia (Littoral) and 95 kWh/(m^2 y) in Latvia.

In accordance with the Technical Conditions in Poland [3], buildings in Poland should be designed in such a way that the value of the partial PE index for heating, ventilation, and hot water preparation for a single-family house does not exceed 70 kWh/(m^2 y), and for a multi-family residential building 65 kWh/(m^2 y). This requirement in 2014 was 120 and 105 kWh/(m^2 y), respectively. The partitions and technical equipment of the building must meet at least the thermal insulation requirements specified in the regulation.

A Long-Term Renovation Strategy [4] was adopted in Poland in February 2022 under Directives 2010/31 and 2018/844 [5]. It aims to ensure high energy efficiency and low carbon building stock by 2050 while cost-effectively converting existing buildings into nearly zero-energy buildings. There are 14.2 million buildings in Poland, many of which are characterized by low energy efficiency and will require renovation in the coming years. In the case of multi-family residential buildings, after 2020, 30 % will still require thermal modernization. At the same time, this share may increase further under the influence of the upward trend in the prices of energy carriers. In 2020–2030, 236,000 buildings are planned to be thermo-modernized annually. In the following years, 2030–2040 – 271,000 buildings; in the years 2040–2050 – 244,000 buildings; and in 2021–2050 – 7.5 million, thermal modernization is expected.

Thermal modernization activities include, in particular:

- Insulation of external partitions (roofs, walls, floors on the ground, and ceilings above the cellars).
- Replacement or modernization of window and door joinery, installation of door closers,
- Application of heat recovery in ventilation systems.
- Use of ventilation control devices (diffusers, mechanical exhaust ventilation).
- Application of solutions that reduce the need for cooling in the summer.
- Application of solutions enabling passive and active optimization of the use of solar radiation in the winter and prevention of overheating of rooms in the summer.

By 2019, thermo-modernization works were carried out in Poland in 30 % of multi-family buildings subjected to Central Statistical Office (GUS) research. The most popular thermo-modernization activity was the insulation of the external walls of buildings (93.0 %); only in part (36.5 %) of the modernized buildings' windows or doors were replaced. Actions aimed at technical equipment of buildings were chosen less frequently: heat source or heat substation (modernization or replacement of the heat source – 12.5 %, modernization of the substation – 14.3 %, modernization of the internal heating system – 25.2 %, modernization of the domestic hot water installation – 13.3 %, modernization or replacement of ventilation installation – 5.6 %, modernization of the lighting system in the common parts of the building – 22.5 %. It is estimated that thermal modernization is profitable in a significant part of buildings in the current market conditions. The transition towards climate neutrality by 2050 means several gradual changes in the area of energy carriers used: a complete abandonment of the use of coal for heating purposes and an almost complete phase-out of the use of natural gas in buildings. In buildings where a heat pump has been installed due to deep thermal modernization, the target final energy ratio for heating, ventilation, and domestic hot water preparation should be no more than 30 kWh/(m^2 y).

Economically viable thermal modernization potentially allows to obtain:

- Final energy savings in residential buildings of up to 147 TWh, which amounts to approximately 75 % of the current level of their final energy demand in Poland.
- Reduction of CO_2 emissions by over 37 million tons per year, which is about 10 % of the total annual greenhouse gas emissions in Poland.
- The reduction of dust emissions by about 89,000 tons per year is about a quarter of the total dust emissions in Poland.

1.1. State-of-art

TRNSYS is a flexible energy simulation software widely used for energy analysis of buildings, and solar energy systems including the vast amount of components for thermal and electrical energy systems. Rabani et al. [6] proposed an optimization method for automating the procedure of minimizing the energy consumption of the building and achieving the NZEB target. In the study, indoor climate and energy simulation and a generic optimization tool are used to optimize energy use in a building located in Norway. Visual and thermal comfort criteria are studied, considering energy supply, fenestration and shading. The optimization results show that energy usage of the building can be decreased by up to 77 % and enhance thermal comfort.

Hong et al. [7] strived to identify optimal retrofit solutions for Shanghai's low-rise buildings. An optimization approach is used, integrating life cycle cost and an environmental evaluation. The study is coordinated with on-site surveys, modelling, and data analytics. The results show that improvement in heating and cooling systems and integration of renewable energy systems are the primary measures to attain maximum life cycle.

Want et al. [8] developed a framework for retrofitting existing buildings to NZEB. The proposed framework is implemented in a building located in Beijing. The reliability and practicability of the system are investigated. Results show that before the retrofitting, the building's electricity consumption was 23,739.1 kWh/y. Once the framework is implemented, the electricity consumption of the building is reduced to 14,033.1 kWh/y.

Fina et al. [9] determined the optimal size of various technologies for renewable energy for buildings. In order to maximize the net present value, a mixed-integer linear programming optimization model is proposed. The results indicate that the proposed method can achieve a profitability ranking of different energy sources and economic rationality of investments in various heating and electricity technology.

Rafał et al. [10] studied the effect of using photovoltaic micro-installations in single-family buildings in Poland and other countries in Eastern and Central Europe. The authors selected the Małopolska Voivodship area of Poland for the study due to the low air quality and the high density of single-family buildings. The conclusions show that using photovoltaic micro-installations reduces CO_2 generated by three power plants and combined heat and power plants under consideration by 1.17 %.

Godin et al. [11] investigated the structural barriers to NZEB in lower-income and rural jurisdictions in a developed country. The proposed method suggested that the cost and demand of NZEB are the most significant barriers to the energy transition.

Therefore, the EU is dealing with a sharp increase in electricity, gas, oil, and coal prices. The implementation of energy-saving technologies, systems reducing energy consumption, and thermo-modernization becomes not only an element of climate policy but an inevitable economic necessity.

Different tools can analyze the behavior of the buildings, such as TRNSYS, IDA, ICE, or EnergyPlus. Mazzeo et al. [12] evaluated the prediction accuracy of the software by means of comparing experimental results with simulation results. In this article, TRNSYS software is used as it is a powerful tool for commercial and residential building simulations and is extensively used for the transient simulation of thermal systems. TRNSYS environment essentially has two cores; the first part consists of a components library, including heating, ventilation and air conditioning (HVAC) units, hydronics, controllers, solar thermal systems, and storage systems. In contrast, the second part is based on an engine that processes the input files and solves the system equations iteratively.

Quesada et al. [13] prepared a dynamic model for 7.2 kWp photovoltaic (PV) installation under standard test conditions (STC) using TRNSYS software. The dynamic model is validated from the data collected during an experimental study. The experiments are conducted with forty-two PV modules and three inverters with a data acquisition system. In system modeling, two different approaches are used. The difference in approaches is the weather data used in the simulations. PV power output calculations in the first system are performed using meteonorm weather data. In contrast, collected in-field weather data is used in the second system. The total PV electricity production was 16.93 MWh experimentally, whereas the value was 17.41 MWh (2.8 %), predicted by the TRNSYS model.

Kenai et al. [14] integrated extensive green walls (GWs) on the wall of a brick house located in Lille, France. The building analyzed consists of two floors with a total area of 100 m^2. GWs are placed on the south and west side of the building. Ivy and Virginia Creeper are used as GWs in the study. The effects of GWs during dynamic thermal calculations are evaluated using the TRNSYS software. The results show that GWs are able to protect the facades against overheating and reduce the energy consumption for air conditioning in summer. The interior temperature difference was 7.5 °C when compared GWs to the conventional wall. During the winter, GWs can benefit from solar irradiation and reduce the heating demand.

The TRNSYS software contains various heat pump models. The models rely on the user-supplied catalog data containing normalized heating capacity, power consumption, load, and source side flow rates. Therefore, extensive performance mapping is required to model the heat pump accurately. Bordignon et al. [15] proposed a new TRNSYS Type based on user-defined data containing the coefficients of compressor polynomials, characterizing the heat pump compressor's operating conditions. The proposed model can simulate reversible ground source water-to-water heat pumps with different configurations and refrigerants. The new model is tested for a ground source heat pump for three different climatic conditions. The COP is 3.29, 3.61, and 4.90 for Helsinki, Strasbourg, and Athens, respectively.

Eddib et al. [16] conducted an energy analysis for an apartment with an 85 m^2 floor area located in Tangier, Morocco. The hygro-thermal behaviors of the multi-zone apartment are evaluated using TRNSYS software. The heating energy demand for keeping the zones at 18 °C is found and validated to be 160 kWh for winter. The 540 kWh cooling energy demand to preserve 25 °C in zones over the summer.

Potočnik et al. [17] strived to improve thermal comfort in residential buildings using a smart control algorithm and optimized weather-controlled air-to-water heat pump. A two storeys single-family building with two zones is investigated. A generalized weather-dependent heating temperature function is proposed. The authors concluded that instantaneous solar irradiation significantly enhances thermal comfort when optimized into a parametrized solution to control the heat pump.

Mansir et al. [18] developed a TRNSYS model to investigate the transient behavior of energy systems to cover the heating and electricity demand for residential buildings. A hydrogen fuel cell/electrolyzer energy storage and battery systems are studied comparatively, taking economical and environmental aspects into consideration. A residential building is modelled considering ASHRAE standards with a total residential area of 135 m^2. The results show that the capital cost of the hydrogen system is twice the cost of the battery system for an HVAC system. The battery system showed less-effective performance when used for higher loads.

Belmonte et al. [19] conducted research on the performance of a solar-assisted heat pump system (SAHP), including a phase-change storage tank for a single-family house located in Madrid, Spain. An experimentally validated horizontal slab-like macro-encapsulated phase change material (PCM) tank model is implemented in TRNSYS software. The simulation results show that implementing the PCM tank to the SAHP system generated degradation in the system performance. The use of conventional control strategies led to the diminishing of the solar energy transferred to the heat pump by around 30 %.

Yuan et al. [20] proposed a hybrid energy system based on solar energy for a residential neighbourhood with 14 eight-storey buildings with 31,100 m^2 of floor area. The system consists of PV modules, air-to-water and water-to-water heat pumps, a buffer tank, and a borehole heat exchanger. In the system, the heat generated by solar collectors is stored in borehole heat exchangers during the non-heating season. The results indicated that 38–58 % of the total heating demand could be covered with the energy cost of 110–184 €/MWh. The capital cost of the proposed system is higher than district heating. However, the solution is able to reduce CO_2 emissions by 102–217 tons.

Endo et al. [21] designed a hydrogen energy utilization system with renewable energy comprising a 20 kW PV system, an electrolyzer, a fuel cell, a hydrogen storage tank, and a battery. A small building was chosen to construct a zero-emission system. The 48 h of operation is considered where the first day is sunny and the second day is cloudy. The simulation results were in agreement with the actual operation results obtained from the constructed system. The main discrepancies between actual and simulation results were due to the charge–discharge of batteries during hydrogen production.

Rashad et al. [22] studied heat transfer through the envelope, energy demand, and thermal comfort for a three-zone building using TRNSYS software. A correct way of determination of the energy demand and cost-effective renewable energy source installation are discussed.

Hernández-Arizaga et al. [23] conducted research to model thermal facilities to develop energy improvement techniques. The thermal facility is located in a building with 26 apartments in Durango, Spain. The energy analysis is carried out by combining TRNSYS and MATLAB software to calibrate the model iteratively. A methodology is proposed to validate the model based on data acquired from the supervisory control and data acquisition (SCADA) and overcomes the limited data difficulties.

Baldinelli et al. [24] proposed an environment-adaptive wall characterized by drowning pipes on the wall's inner and outer surfaces and can change the wall's thermophysical properties dynamically. The concept of the adaptive wall is based on floor radiant panels. Different configurations of the pipe structures, such as sparse-serpentine, sparse-counterflow, and dense-counterflow, are analyzed. The environment-adaptive wall is then implemented in TRNSYS software and studied for different cities located in various climatic zones. The results indicated a reduction of more than 50 % of energy losses and gains in moderate climate conditions, notably in hot seasons.

Lin et al. [25] investigated the thermal performance of a semi-nested building coupled with an earth-to-air heat exchanger to improve indoor thermal comfort and decrease the energy consumption of the building. The building and the energy system model are implemented in TRNSYS software and validated using the results from the literature. The Taguchi iteration method is used to find optimal design parameters. The optimal design is capable of maintaining indoor temperatures between 18.9 °C and 26.04 °C with 70.1 % of energy savings.

Açıkkalp et al. [26] studied a photovoltaic/thermal (PV/T) based air-cooling system for a building using TRNSYS software located in Izmir, Turkey. A single-zone lumped capacitance building model with a 90 m^2 surface area is analyzed, and an extended exergy analysis is conducted. 0.84 and 0.18 maximum exergy efficiencies are obtained for conventional and extended exergy analyses, respectively.

Mehmood et al. [27] strived to determine the best resilient cooling solutions for buildings in hot countries to increase heat resilience capacity. A parametric analysis is conducted by considering the impact of climate change on cooling demand and indoor thermal comfort in extremely hot, dry climates of southern Asia, Pakistan. The building's

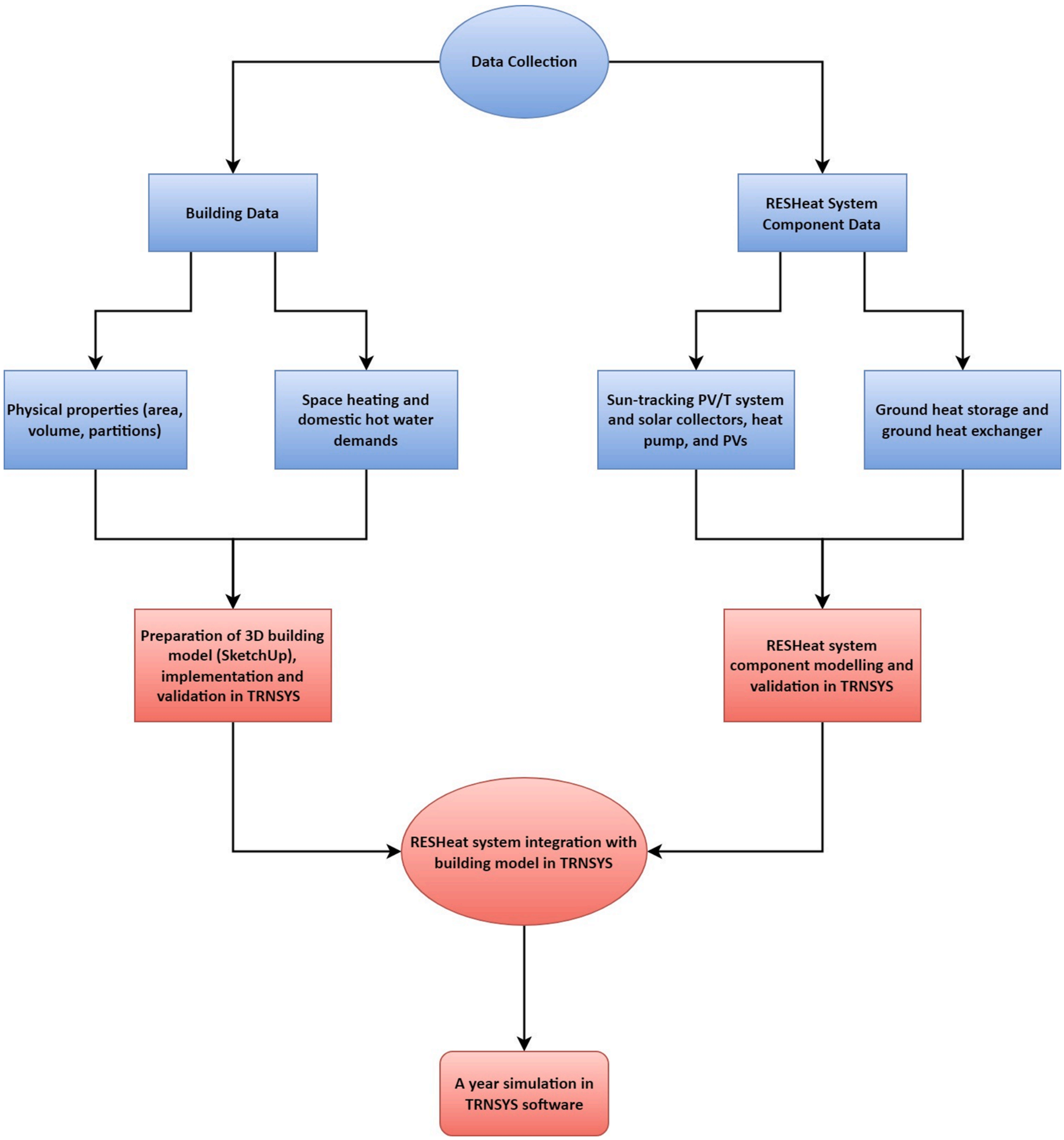

Fig. 1. Flowchart of the performed analysis.

cooling needs and thermal comfort conditions are studied by taking into account ASHRAE criteria using the TRNSYS tool. The research results show that the annual cooling demand is forecasted to increase between 20.56 and 66.96 kWh/m^2 and the increase in thermal discomfort hours ranging from 423 to 1,267 h by 2,080. Passive cooling measures are highlighted to increase energy savings and reduce thermal discomfort hours.

Naji et al. [28] investigated the effects of the envelope on a prefabricated building's energy demand, thermal comfort, and daylighting levels for six different climatic zones in Australia. The building model analyzed has a total floor area of 214 m^2 and 15 thermal zones. A regression-based sensitivity analysis is conducted to acquire the most sensitive parameters using TRNSYS. The results indicated that shading and window glazing are the most influential parameters.

Sakellariou and Axaopoulos [29] developed a new energy performance metric for solar-assisted ground heat pump systems (SAGSHP) with the utilization of PV/T. The number of PV/T modules and the inclination of the PV/Ts are varied for two different topologies of SAGSHP. The dwelling under consideration had a space heating demand of 3,522 kWh annually at 20 °C in heating zones and domestic hot water demand of 2,528 kWh at 50 °C. The novelty of the proposed metric is that the method accounts for the electrical energy produced by PV/T modules. The results show that the proposed method is capable of performing energy analysis for systems equipped with PV/Ts via a holistic perspective.

Kavian et al. [30] studied a residential building with seven thermal zones and three floors located in Tehran, Iran. The maximum heating load of the building is 13.22 kW, whereas the maximum cooling demand is 17.66 kW. The hybrid solar PV and ground source heat pump (GSHP) system is integrated to analyze energy, exergy, economic and environmental impacts using the TRNSYS tool. Multi-objective optimizations of the life cycle are conducted using a particle swarm optimization algorithm. The conclusions show that polycrystalline PV surfaces can provide 31 % of the solar factor.

Numerous negative consequences arise because of the global population and the environmental impacts of greenhouse gas (GHG). The

Table 1
Properties of the partitions of the building.

Partition	Thickness, m	U, W/($m^2 \times K$)
External wall	0.39	0.22
External non-insulated roof	0.04	2.90
Ceiling above the last floor	0.33	0.21
Internal wall	0.28	0.99
Internal ceiling	0.27	0.55
External window	–	1.10

change in climate and low air quality are the two most visible effects of GHG. A major fraction of the energy is consumed by residential buildings in the world. CO_2 emissions from residential buildings reached 10 Gigatonnes in 2019, representing 28 % of global energy-related emissions [20]. Due to the increment in population, the energy consumption of buildings has exceeded the industry sector and become the most prominent consumer globally. In the EU, the building sector consumes 40 % of the total energy. Space heating and cooling and domestic hot water preparation represent 55 % of the total energy consumption [31]. The increment in energy demand and environmental concerns bring forth renewable energy sources.

Ozyogurtcu et al. [32] analyzed four different HVAC systems; (I) a 100 % fresh air system, (II) a 100 % fresh air with half air volume rate at night period, (III) the same as the second system along with heat recovery unit and (IV) 50 % fresh air with half air volume rate at night period with heat recovery and mixing units serving to operation rooms in five different cities in Turkey. The energy analysis for those four systems is conducted along with a life cycle cost (LCC) analysis for 20 years. The authors concluded that heat recovery and mixing units considerably reduce the LCC and energy consumption, especially for locations with extreme climate conditions. The lowest LCC and energy consumption is achieved with the fourth option reducing the energy consumption by 74 % compared to the first option.

The literature review shows that researchers are focused on problems such as glazing and shading to reduce the energy demand of the building for heating and cooling. The most common approach was upgrading the heating system to increase energy efficiency using renewable energy sources, reducing electricity consumption, optimizing the sources and use of renewable energy, and using photovoltaic panel installations to reduce CO_2 emissions. The currently proposed systems for NZEBs lack coverage of both electrical and thermal energy demands and suffer from the high cost of implementation in the literature. In the case of old-type residential buildings, it is necessary to ensure at least 60 °C of fluid temperature to cooperate with radiators, fan-coils, or district heating systems, leading to a decrease in COP.

This paper proposes a solution to cover residential buildings' electrical and thermal energy demand by integrating renewable energy systems and using a developed efficient energy storage system. The Renewable Energy System for Residential Building Heating and Electricity Production (RESHeat) system enables an advanced 100 % RES system on combined cooling, heating, and power (CCHP), including seasonal underground energy storage for residential buildings. One of the proposed system's main novelties is innovative sun-tracked PV/T to improve the energy efficiency of SAHP systems. Another novel idea is to use waste heat from sun-tracked PV/T and sun-tracking solar collectors for ground regeneration (through boreholes drillings and underground storage in the non-insulated tank). The system allows seasonal thermal energy storage in the ground and uses it to increase the COP of the water-to-water heat pump by increasing the fluid load temperature. Ground regeneration is vital through using waste heat from PV panels cooling allows maintaining COP of the heat pump at a constant level over consecutive heating seasons. Therefore, the proposed RESHeat system can leap forward in the energy transition and bring an efficient solution to the energy market.

In this paper, the components of the RESHeat system, such as the heat pump, sun-tracking solar collectors, PV modules, underground thermal energy storage unit, and borehole heat exchanger, are validated using experimental data along with the building model. The article also presents the methodology and describes the model developed in TRNSYS, which will enable a year-round analysis of the system parameters and an accurate estimation of the demand and energy production of the system.

2. Methodology

The research aims to integrate the RESHeat system into one of the demo site buildings. A building model is required to determine the energy demand and integrate the RESHeat system. Modelling the behaviour of a building enables one to make critical decisions during the implementation of new systems or to retrofit the existing one. The integration of the RESHeat system with the building allows one to conduct a response surface study and optimize the system.

One of the most useful components of the TRNSYS library is Type56 which allows multi-zone building modeling using the TRNBuild. This type allows users to divide the model into zones and assign heating and cooling loads, energy gains, humidification, and operating schedules.

A flowchart of performed analysis is given in Fig. 1.

2.1. Energy simulation of the demo site building

The building's location, geometry, and energy characteristic are presented at the beginning of the section. The RESHeat system schematic, components, and the objectives of components are briefly explained. The components are modeled and validated at the end of the section.

2.1.1. Building location

The demo site building is located in a small town in southern Poland. The area has a moderate climate, and the temperature typically varies from −10 °C to 28 °C over the course of the year. The average percentage of the sky covered by clouds experiences significant seasonal variation. The rainy period lasts seven months, and the winters are usually cold, with a mean temperature below 2 °C. The summers are usually warm; 27–28 °C are the typical maximum temperatures in July.

In TRNSYS software, the weather data can be provided in different formats, including typical meteorological year (TMY), TMY2, TMY3, EPW, Meteonorm, and user-defined. The weather data used in the simulations is gathered from the closest weather station.

2.1.2. Building geometry and energy characteristics

The RESHeat system is implemented in only one storey of the building. The storey consists of 9 multi-family apartments. The storey has 33.64 m long and 26.13 m wide, and 2.8 m in height. The nine apartments occupy 433 m^2 of the building. The building envelope partitions properties are given in Table 1.

The demo site is located in zone 3 according to the climatic zones of Poland. The heating system is designed considering an outside temperature of −20 °C according to PN-EN 12831:2006 standards. The storey under the RESHeat system construction has a maximum heat load of 34.37 kW. The domestic hot water usage of the storey is estimated as 41.66 L per hour at 45 °C.

The building heating system consists of two 60 kW gas boilers used for central heating (CH) and domestic hot water (DHW) preparation for the whole building. Central heating radiators are used in apartments. The heating setpoint temperature is 22 °C, and the setback temperature is 20 °C.

The occupancy per apartment is, on average, three. The heat gains from people, lights, and electrical equipment are estimated using the ASHRAE, VDI 2078, and SIA norms. ASHRAE norms indicate that the degree of the person's activity affects the heat generated by the human body. A similar approach is applied in order to calculate the heat gains

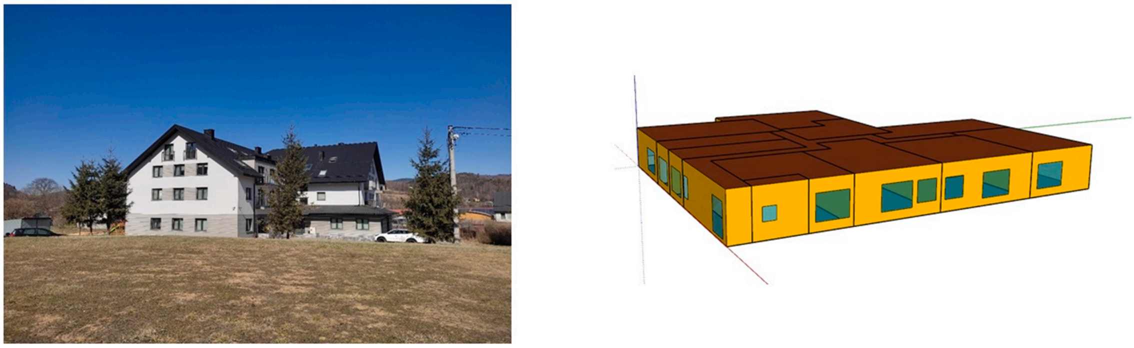

Fig. 2. Geometric model of the storey.

Table 2
Monthly demand of the storey.

Months	CH Demand, MWh/y	DHW Demand, MWh/y
January	7.90	0.90
February	6.46	0.81
March	4.96	0.90
April	2.30	0.87
May	0.57	0.90
June	0.05	0.87
July	0.00	0.90
August	0.05	0.90
September	0.87	0.87
October	2.70	0.90
November	5.09	0.87
December	7.01	0.90

from electrical equipment and lights. TRNBuild allows setting up a schedule for different gains and losses. It is assumed that residents work between 8 a.m. and 4p.m. The lighting schedule is arranged to work between 6 a.m. and 8 a.m. and 4p.m. and 11p.m.

The air infiltration depends on the type of rooms of the apartments. Air changes per hour for bedrooms, living rooms, bathrooms, and corridors are 0.5, 1, 2, and 1.5, respectively, according to Heating CIBSE Guide B1: 2016 [33]. The heat loss due to air infiltration can be calculated using Eq (1).

$$\gamma_{air} = \dot{v}_{inf} q_{air} c_p (T_{in} - T_{out}), \quad (1)$$

where $\dot{v}_{inf}$ is the infiltration rate, m^3/s, q_{air} is the density of the air at a mean temperature, kg/m^3. c_p stands for the specific heat capacity of air at constant pressure and mean temperature, $kJ/(kgxK)$. T_{in} and T_{out} are the inside and outside air temperatures in K, respectively.

2.1.3. Building model TRNSYS

In this section, the 3D model of the storey is prepared using the architectural drawings in commercial 3D design software. The design tool has a TRNSYS 3D plugin which allows thermal zone creation. When the storey is modeled, it is exported to the TRNSYS program with the *.idf extension. The actual building and the created 3D model of the storey are illustrated in Fig. 2.

The created storey model is validated using the maximum heating load of 34.37 kW. In TRNSYS software, the environment and weather parameters are arranged by considering PN-EN 12831:2006 standards. The maximum heating load of the model is found to be 34.98 kW. The percentage error between the actual data and the model is 1.79 %. Once the model is validated, the yearly heating and domestic hot water demand of the storey are calculated as 37.96 MWh/y and 10.62 MWh/y, respectively. The monthly central heating and domestic hot water demand of the storey is given in Table 2.

The summary of the energy demand of the storey is shown in Fig. 3.

3. Component models and validations

The RESHeat system is currently being implemented at this demo site. The schematic of the RESHeat system installation is shown in Fig. 4. Five sun-tracking solar collectors (SC) are installed at this demo site to

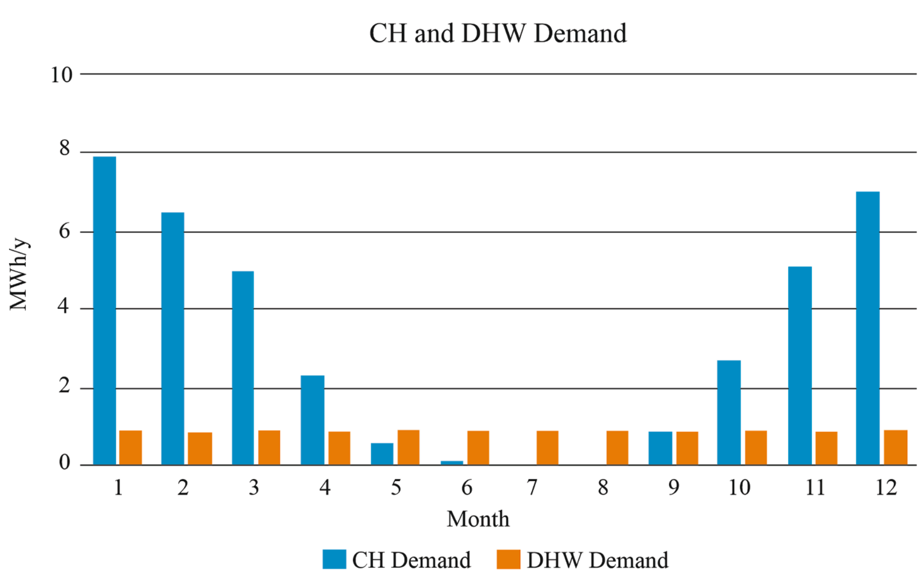

Fig. 3. The summary of energy demand.

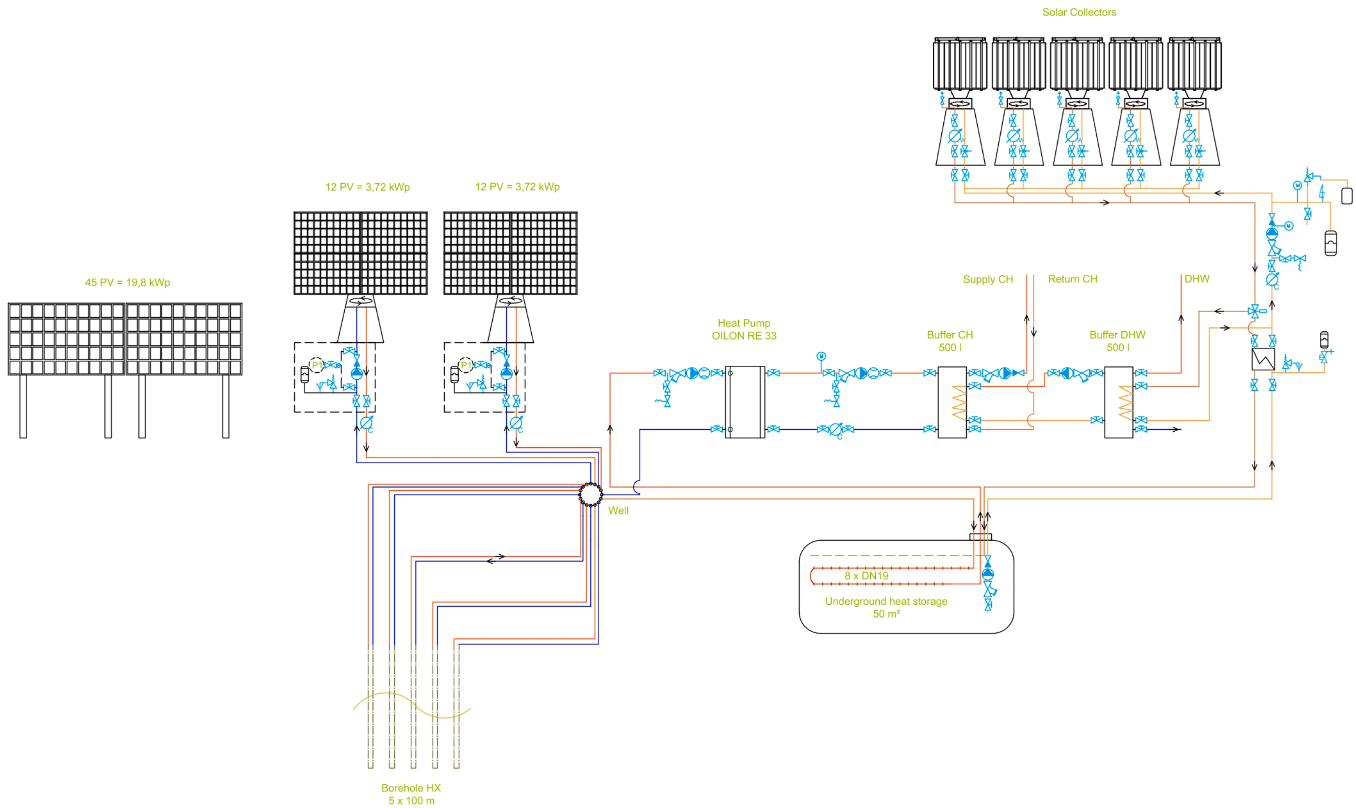

Fig. 4. The schematic of the RESHeat system.

Table 3
Parameters of PV module.

Parameters	NOCT	STC
Short circuit current (I_{SC})	9.05 A	11.44 A
Open-circuit voltage (V_{OC})	46.60 V	50.10 V
Current at maximum power point (I_{MPP})	8.50 A	10.56 A
Voltage at maximum power point (V_{MPP})	38.50 V	41.70 V
Module Power, W	327.6	440
Temperature coefficient of I_{SC}	0.05 %/°C	0.05 %/°C
Temperature coefficient of V_{OC}	− 0.29 %/°C	− 0.29 %/°C
Module Efficiency, %	18.83	20.24

Table 4
PV module model results.

Parameters	NOCT	STC
Short circuit current (I_{SC})	9.05 A	11.44 A
Open-circuit voltage (V_{OC})	46.48 V	49.97 V
Current at maximum power point (I_{MPP})	8.48 A	10.53 A
Voltage at maximum power point (V_{MPP})	38.49 V	41.68 V
Module Power, W	327.4	439
Module Efficiency, %	18.82	20.20

generate thermal energy. The thermal energy will be stored in buffer tanks to cover the central heating and domestic hot water demands. The excess heat from the solar collectors will be stored in an underground heat storage tank during the non-heating season. The specially designed underground storage tank with a 50 m^3 capacity is used. The accumulated thermal energy is further utilized for the heat pump to keep the COP high as possible during the heating season.

Forty-four stationary photovoltaic panels are installed to harvest electrical energy to cover the electricity consumption of the heat pump and also the consumption of the control and overall RESHeat system. Two sun-tracking PV/T systems, each consisting of 12 PV modules, are installed to support electricity generation. The produced low-temperature thermal energy will be stored in the borehole heat exchanger. The low-temperature thermal energy will be used during the winter to keep the COP of the heat pump as high as possible.

A water-to-water heat pump with a heating capacity of 42 kW is used. Five each 100 m depth borehole heat exchangers are used to store the excess thermal energy during the non-heating season and harvest it back during the heating season for the source side of the heat pump.

Each component used in the system is modeled and validated in TRNSYS software using data acquired from the SOPSAR project funded by Polish National Centre for Research and Development between 2018 and 2021.

3.1. Photovoltaic module model and validation

A TRNSYS library component, Type 103b, suitable for modeling the electrical performance of mono and polycrystalline PVs, is used to model the PV system. The four-parameter model, which assumes that the slope of the current–voltage characteristic is zero at the short-circuit condition, is used to model Type 103b. The manufacturer data is studied, and the model is simulated under STC and normal operating cell temperature (NOCT) conditions. The parameters of the 440 W module are given in Table 3.

The PV module has an area of 2.17 m^2 and 144 cells in series. The NOCT temperature for the module is 44 °C ∓ 2 °C.

The weather data such as ambient temperature, beam radiation, ground reflected diffuse radiation, diffuse sky radiation, array slope, and incidence angle of beam radiation are provided using NOCT conditions and STC. The model results are given in Table 4.

The module power estimation error was 0.06 % and 0.22 % for NOCT and STC conditions, respectively.

Table 5
Parameter of the solar collector.

Parameters	NOCT
Collector gross area, m^2	5.376
Fluid specific heat, kJ/(kg × K)	3.7
Flow rate at test conditions, kg/(h × m^2)	33.48
Optical efficiency	0.611
Heat loss coefficient, W/(m^2 × K)	0.6
Temperature-dependent heat loss coefficient, W/(m^2 × K^2)	0.0053

Table 6
Water-propylene glycol mixture properties.

Water-propylene glycol (35 %)	Value
Fluid specific heat, kJ/(kg × K)	3.70
Fluid density, kg/m^3	1024.33
Fluid viscosity, kg/(m × s)	2.71×10^{-3}
Fluid thermal conductivity, W/(m × K)	0.43

3.2. Sun-tracking solar collector model and validation

The solar collector model is created using Type 1345 from the TRNSYS-TESS library. The weather and solar collector data collected during the SOPSAR project are used to validate the model. The parameters of the solar collector are given in Table 5.

The weather and the inlet temperature of the solar collector data from 06.07.2020 are obtained and used as the input to the model. Water-propylene glycol (35 %) mixture is used as the working fluid in the PV/T system. The working fluid properties are given in Table 6.

The actual and simulation outlet temperature and thermal energy production are compared in Fig. 5 and Fig. 6.

In Fig. 5, T_{real_out} and T_{sim_out} represent the solar collector's actual and simulation outlet temperatures.

In Fig. 6, Q_{real_out} and Q_{sim_out} indicate the actual and simulation thermal energy production of the solar collector. In order to combine the system with the sun-tracking system, Type 15 is used. This type has four different modes as 1 = fixed surface (no tracking), two = the surface rotates about a vertical axis in order to track the sun, three = the surface rotates about a fixed (user-defined) axis, four = the surface 2-axis tracks such that the beam radiation is always normal to the surface. Mode 4 is chosen for the modeling of the sun-tracking system.

The average percentage error for the outlet temperature is 0.71 %. In contrast, the error for thermal output is 3.77 % in the created solar collector model.

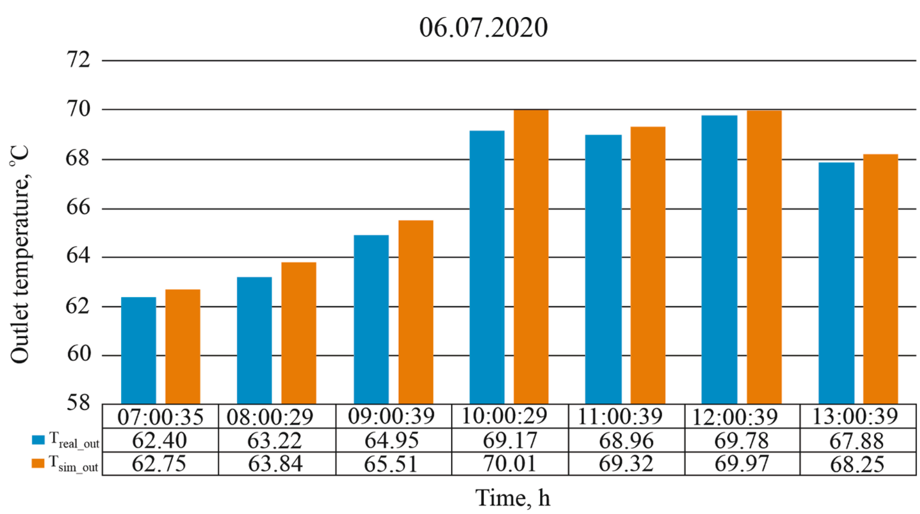

Fig. 5. The outlet temperature comparison.

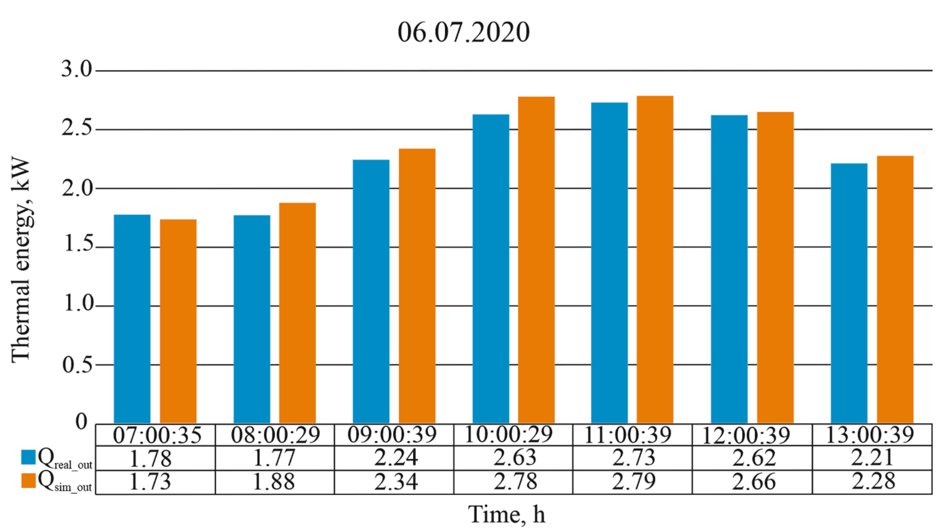

Fig. 6. The thermal energy comparison.

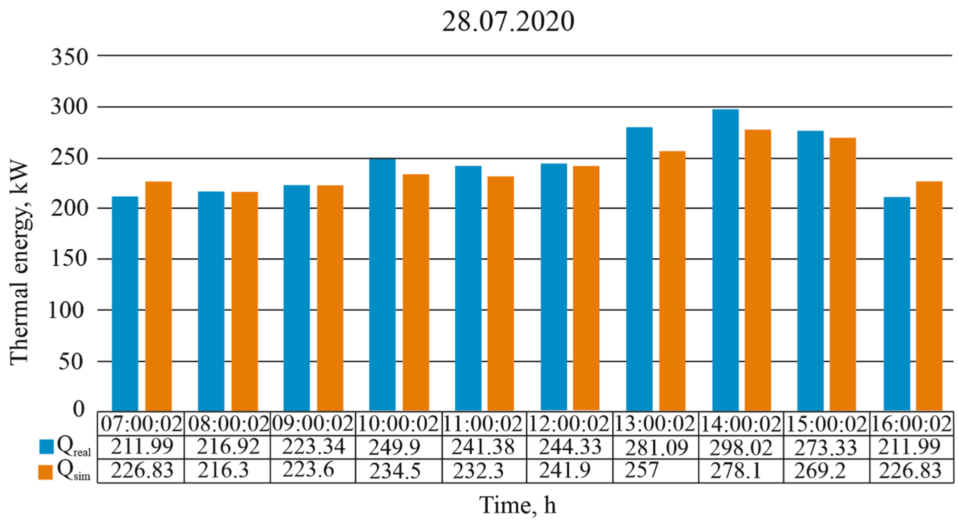

Fig. 7. Thermal energy generation comparison of PV/T system.

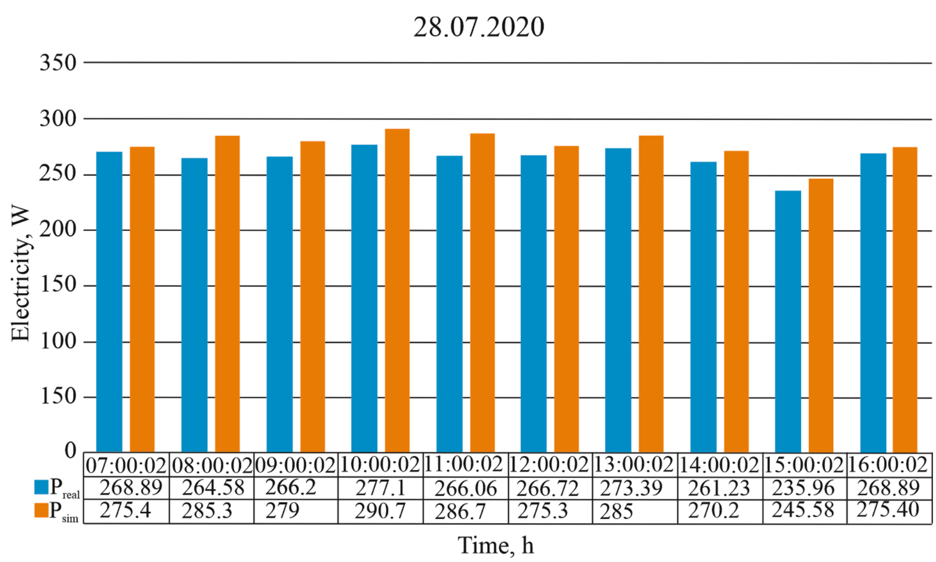

Fig. 8. Electricity generation comparison of PV/T system.

Table 7
Tank properties.

Parameters	Value
Number of ports	1
Tank volume, m^3	50
Tank length, m	8
Fluid specific heat, kJ/(kg × K)	4.19
Fluid density, kg/m^3	1000
Fluid thermal conductivity, W/(m × K)	0.6
Fluid viscosity, kg/(m × s)	8.92×10^{-4}
Loss coefficient (edges, top, bottom), W/(m^2 × K)	6
Heat exchanger (HX) fluid specific heat, kJ/(kg × K)	3.70
HX fluid density, kg/m^3	1024.33
HX fluid thermal conductivity, W/(m × K)	0.43
HX fluid viscosity, kg/(m × s)	2.71×10^{-3}
Inner tube diameter, mm	14.50
Outer tube diameter, mm	19
HX wall thermal conductivity, W/(m × K)	0.4
Length of coiled tubes, m	6
Number of tubes	16
Coil pitch, mm	70

3.3. Sun-tracking PV/T system model and validation

The sun-tracking PV/T system consists of 12 PV modules with a cooling system implemented rear side of each panel. The weather data, inlet temperature for the cooling system, and the flow rate are obtained from 28.07.2020. In TRNSYS solar thermal collector library, Type 50 was chosen to model the PV/T system. In order to achieve the sun-tracking system inside the weather data component of the TRNSYS model, the tracking mode is changed to the surface dual-axis tracking such that the beam radiation is always normal to the surface. Water-propylene glycol (35 %) mixture is used as the working fluid in the PV/T system. The model created in TRNSYS software is validated by comparing the thermal energy generation and electricity production of the PV/T module.

In Fig. 7, the actual thermal energy of the PV/T system is compared with the results obtained from simulations. Q_{real} and Q_{sim} are the actual and simulation thermal energy results.

In Fig. 8, the electricity generation of the PV/T system is compared. P_{real} and P_{sim} are the actual and simulation electricity generation results.

The average error in thermal energy and electricity generation is 4.06 % and 4.74 %, respectively.

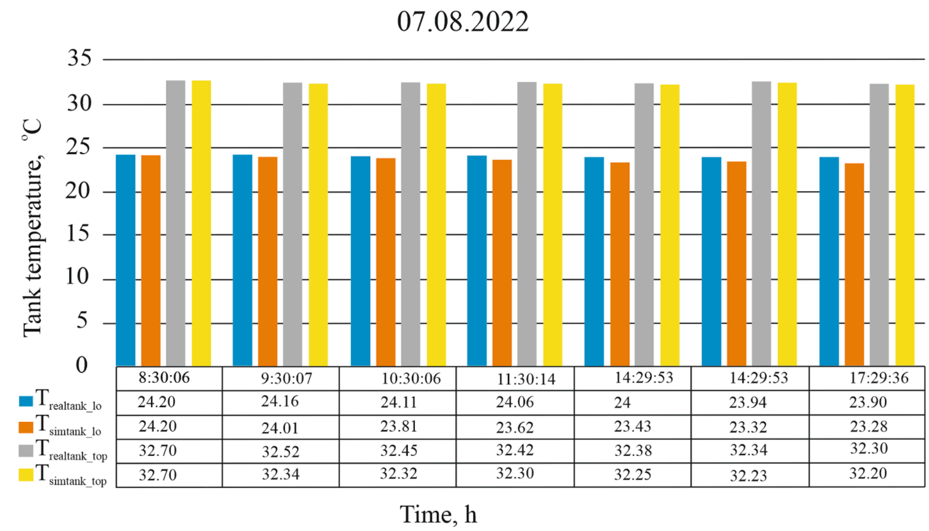

Fig. 9. The comparison between actual data and simulation results.

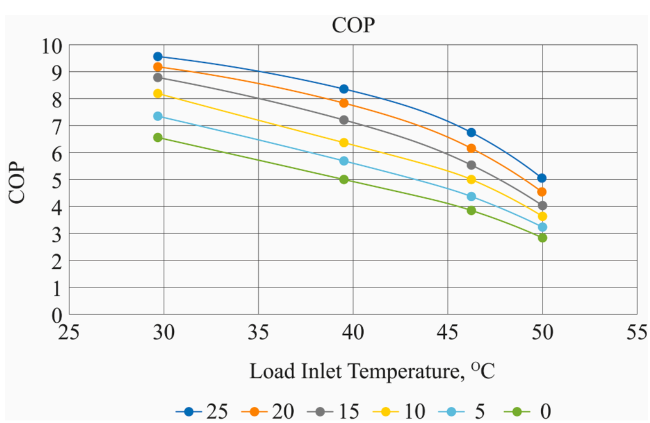

Fig. 10. The COP curve.

Table 9
The heating capacity comparison.

	Load Outlet	60 °C	54.7 °C	48.0 °C	37.6 °C
	Load Inlet	50 °C	46.3 °C	39.5 °C	29.7 °C
Source Outlet	Source Inlet	Actual Heating Capacity / Model Heating Capacity (kW)			
20 °C	25 °C	61.40 / 61.45	62.00 / 61.91	63.60 / 63.76	64.40 / 64.22
15 °C	20 °C	55.80 / 55.90	56.30 / 56.36	56.90 / 56.83	57.60 / 57.75
10 °C	15 °C	50.60 / 50.82	51.40 / 51.28	51.20 / 51.28	51.20 / 51.28
5 °C	10 °C	46.20 / 46.20	45.90 / 45.74	45.60 / 45.74	45.10 / 45.28
0 °C	5 °C	42.00 / 42.04	41.00 / 41.12	40.50 / 40.66	39.70 / 39.73
−5°C	0 °C	37.60 / 37.42	37.00 / 36.96	36.10 / 36.04	35.00 / 35.11

Table 8
The COP comparison.

	Load Outlet	60 °C	54.7 °C	48.0 °C	37.6 °C
	Load Inlet	50 °C	46.3 °C	39.5 °C	29.7 °C
Source Outlet	Source Inlet	Actual COP / Model COP			
20 °C	25 °C	5.10 / 5.13	6.80 / 6.79	8.40 / 8.37	9.60 / 9.52
15 °C	20 °C	4.60 / 4.61	6.20 / 6.18	7.90 / 7.84	9.30 / 9.25
10 °C	15 °C	4.10 / 4.11	5.60 / 5.55	7.20 / 7.20	8.90 / 8.93
5 °C	10 °C	3.70 / 3.69	5.00 / 4.95	6.40 / 6.43	8.20 / 8.24
0 °C	5 °C	3.70 / 3.69	4.40 / 4.39	5.70 / 5.71	7.40 / 7.40
−5 °C	0 °C	2.90 / 2.88	3.90 / 3.89	5.00 / 4.97	6.60 / 6.69

Table 10
Electricity consumption comparison.

	Load Outlet	60 °C	54.7 °C	48.0 °C	37.6 °C
	Load Inlet	50 °C	46.3 °C	39.5 °C	29.7 °C
Source Outlet	Source Inlet	Actual Electricity Cons. / Model Electricity Cons. (kW)			
20 °C	25 °C	12.04 / 11.99	9.12 / 9.12	7.57 / 7.62	6.71 / 6.75
15 °C	20 °C	12.13 / 12.12	9.08 / 9.12	7.20 / 7.24	6.19 / 6.25
10 °C	15 °C	12.34 / 12.37	9.18 / 9.24	7.11 / 7.12	5.75 / 5.75
5 °C	10 °C	12.49 / 12.49	9.18 / 9.24	7.13 / 7.12	5.50 / 5.50
0 °C	5 °C	12.73 / 12.74	9.32 / 9.37	7.11 / 7.12	5.36 / 5.37
−5 °C	0 °C	12.97 / 12.99	9.49 / 9.49	7.22 / 7.24	5.30 / 5.25

3.4. Non-insulated underground storage tank model and validation

Type 1533 from the Solar Thermal Storage-TESS library is used to model the non-insulated underground storage tank, along with Type 77 to model the soil around the tank. The inlet temperature, soil temperature around the tank, flow rate, and the initial bottom and top tank temperature data are collected from 07.08.2022 to validate the model. The properties of the tank are given in Table 7.

The tank is divided into 13 nodes, and each node initialized with the temperature is taken from the real data. The model is simulated for 8 h. The actual bottom and top tank temperatures are compared with the

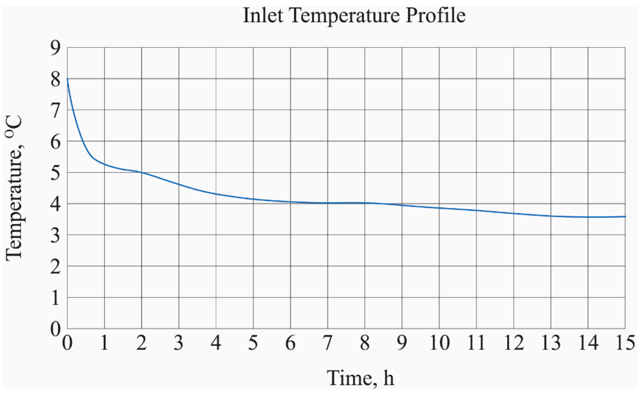

Fig. 11. The inlet temperature profile of the borehole heat exchanger.

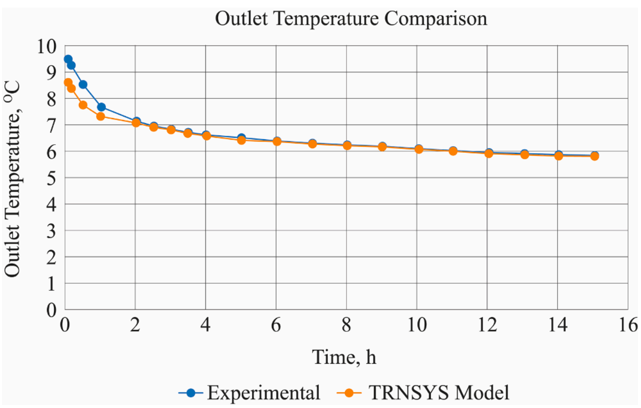

Fig. 12. The outlet temperature comparison of the borehole heat exchanger.

simulation results in Fig. 9.

In Fig. 9, $T_{realtank\_lo}$ and $T_{realtank\_top}$ are the actual temperatures at the bottom and top of the tank. $T_{simtank\_lo}$ and $T_{simtank\_top}$ stand for temperatures at the bottom and top of the tank obtained from the simulation. The average error between the actual data and the simulation results is 0.98 %.

3.5. Heat pump model and validation

In TRNSYS, Type 1323 was chosen from the HVAC library to validate the heat pump. The COP curve of the heat pump is shown in Fig. 10. The heat pump model uses a water-glycol (35 %) mixture as a source-side fluid, whereas the load-side fluid is the water.

The heat pump models rely on the user-supplied catalog data containing normalized heating capacity, power consumption, load, and source side flow rates in TRNSYS. A performance mapping for the heat pump is completed. The actual COP and model COP comparison are given in Table 8. The average percentage error is found to be 0.44 %.

The actual heating capacity is compared to the heat pump model created in TRNSYS software. The results are shown in Table 9. The average error for the heating capacity is 0.22 %.

The comparison between actual and model electricity consumption is given in Table 10. The average error for electricity consumption is 0.34 %.

3.6. Borehole heat exchanger model and validation

The Geothex® ground heat exchanger is validated using the experimental data. The BHE consists of an insulated inner pipe to minimize heat loss between the inner and outer flow channels. In the experiment, a single U-tube borehole heat exchanger is used with a depth of 44.5 m. A TRNSYS Type548b_v2a is used to model the borehole heat exchanger. The model validated comparing borehole to ground (B2G) data for 15 h. Type 14e is also used to create the inlet temperature profile in the experiment shown in Fig. 11.

After the creation of the inlet temperature profile, the inputs such as

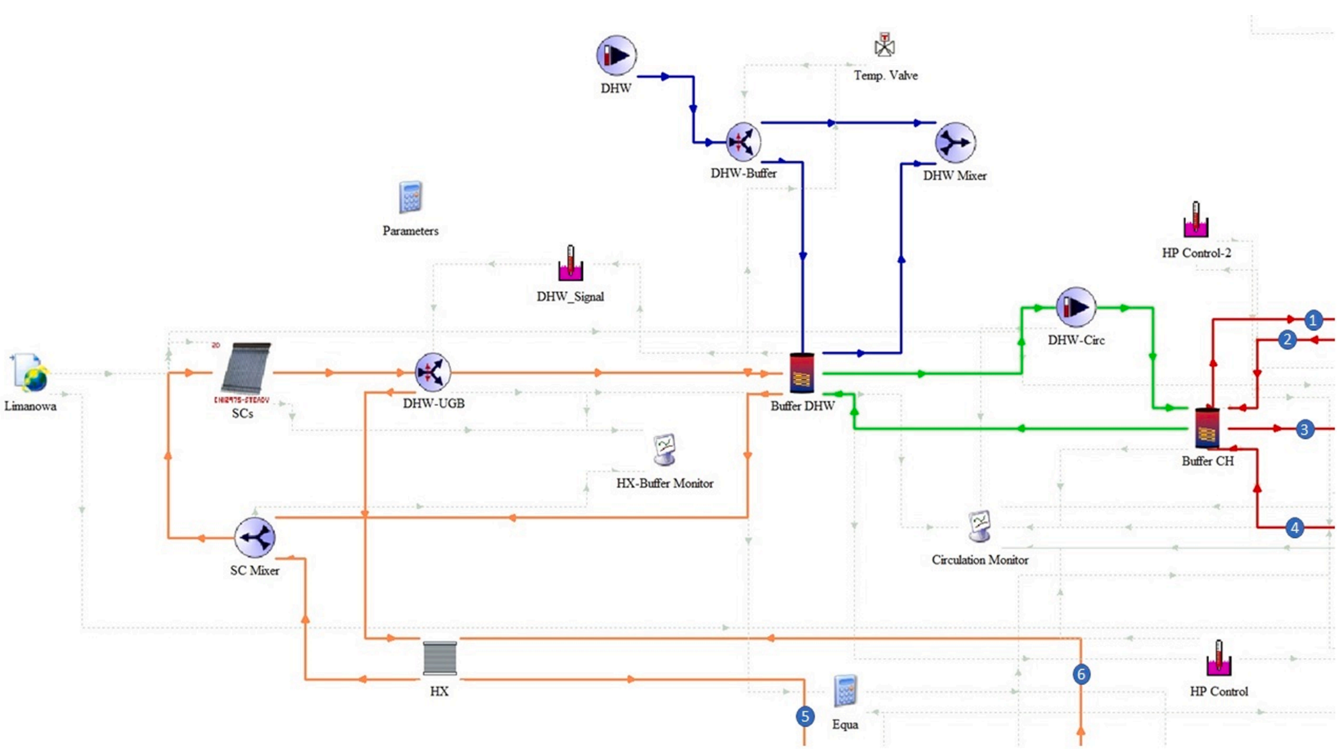

Fig. 13. Solar collector and domestic hot water system.

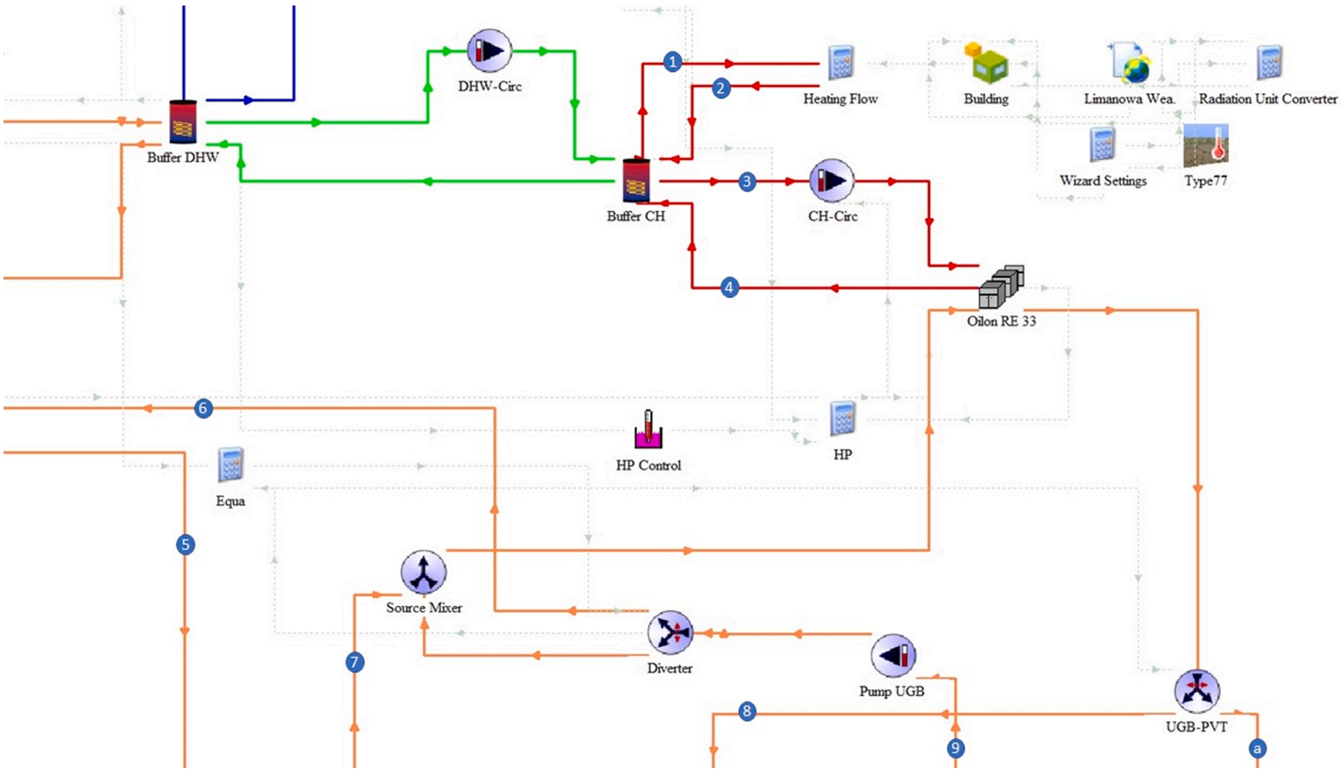

Fig. 14. The central heating and heat pump connections.

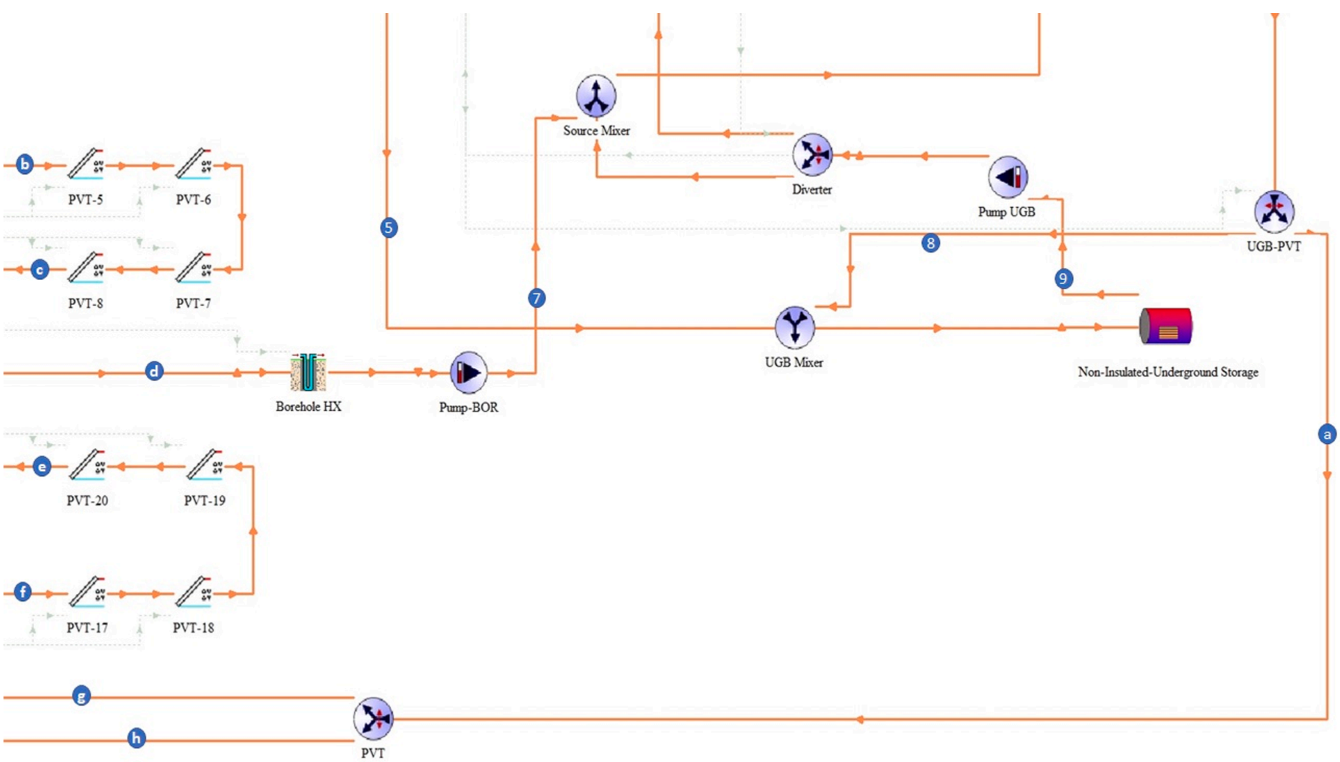

Fig. 15. Borehole heat exchanger and underground heat storage tank connections.

inlet flow rate, flow direction indicator (in order to determine the direction of flow, 1 – circulation from center to border of storage volume, −1 – circulation from border to center of storage volume), the temperature on top of storage which is the temperature of the air directly above the storage volume. In most cases, this is the ambient temperature. At the end of the simulation, the outlet temperature and heat transfer are compared with experimental data. The outlet temperature variation between the TRNSYS model and experimental values is illustrated in Fig. 12.

The average error between the experimental and TRNSYS model

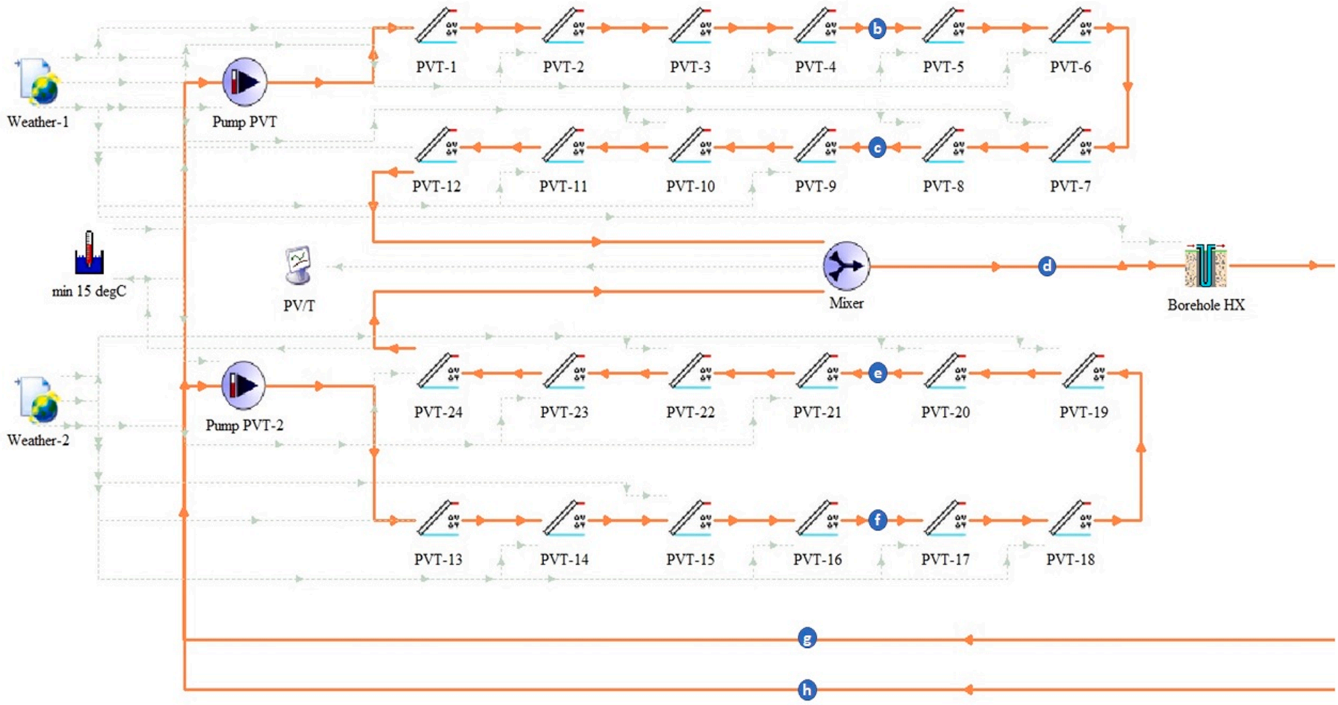

Fig. 16. PV/T system.

Table 11
Summary of the energy analysis.

Generation and Demand	MWh/y
Central heating demand	37.96
Domestic hot water demand	10.62
PV/T thermal energy generation	14.19
Solar collector thermal energy generation	22.65
Heat pump thermal energy generation	42.19
System losses (Controls, pumps, hydraulics)	4.22
PV electricity generation	17.89
PV/T electricity generation	11.74
Heat pump electricity consumption	9.02

outlet temperature is 2.3 %. The heat transfer B2G is 43022.60 kJ for the experimental data. The simulation results show that this value is 42685.04 kJ for the TRNSYS model. Therefore, the error between the experimental data and the TRNSYS model is 0.76 %.

4. The RESHeat system integration with the building model

The system schematic shown in Fig. 4 is used to integrate the system. The transient model of the system is created in TRNSYS software. The solar collector model connection with the buffer tank heat exchanger, along with the domestic hot water preparation, is illustrated in Fig. 13.

The sun-tracking solar collectors are connected to a diverter. When the temperature is 60 °C inside the DHW tank, the water-glycol mixture is diverted to the heat exchanger. The building heating system and heat pump connections are given in Fig. 14. The heat pump is connected to

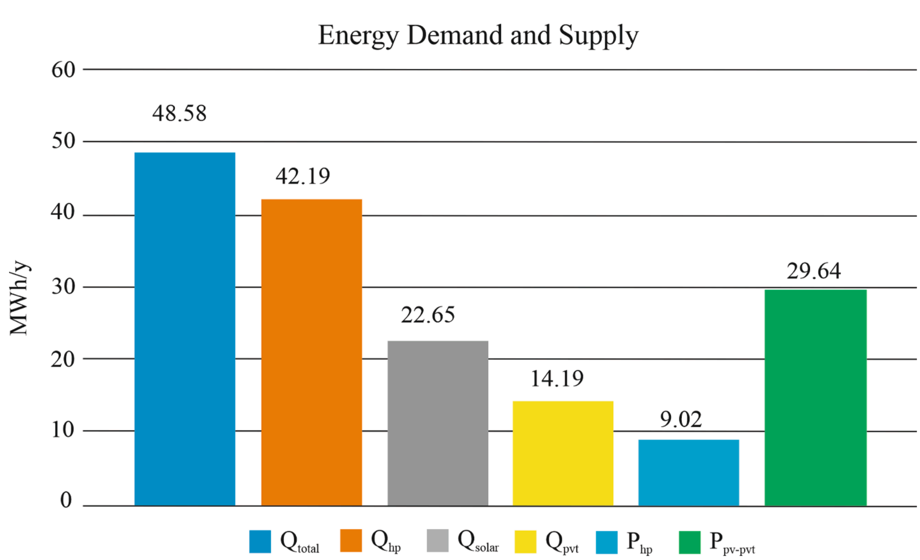

Fig. 17. Energy demand and supply.

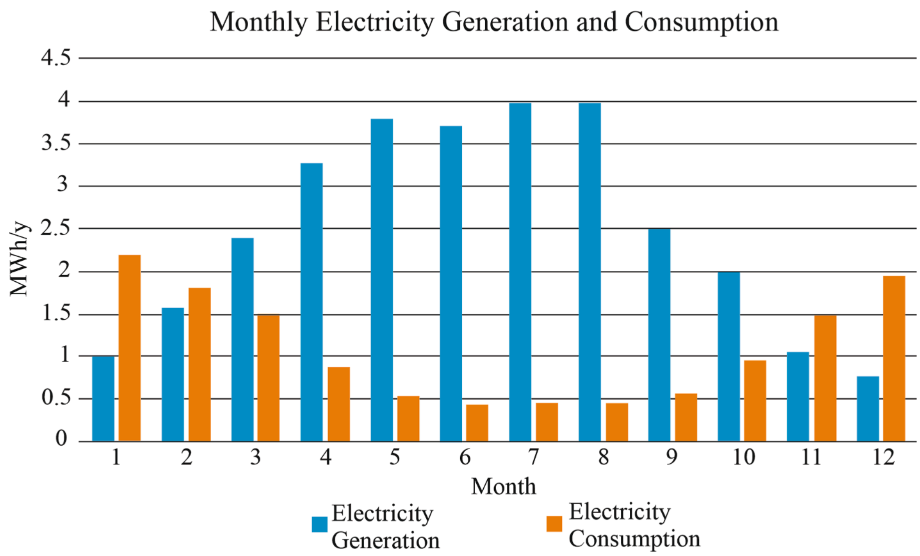

Fig. 18. Monthly electricity generation and consumption.

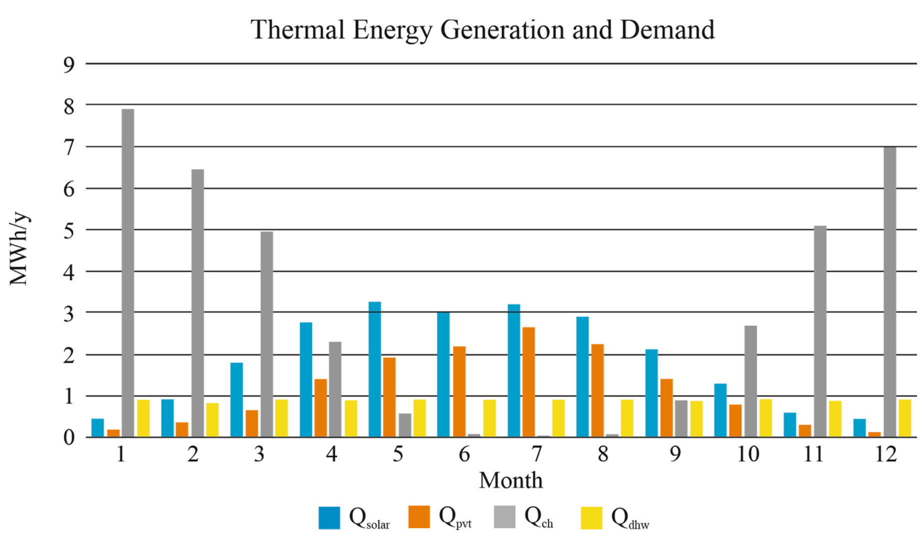

Fig. 19. Monthly solar collector heat generation, along with central heating and domestic hot water demand.

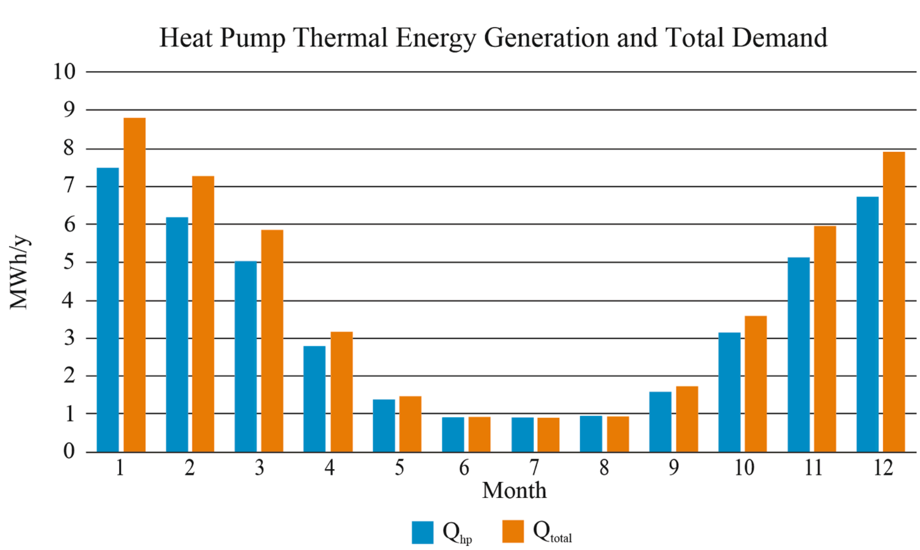

Fig. 20. Monthly heat pump thermal energy generation and total demand of the storey.

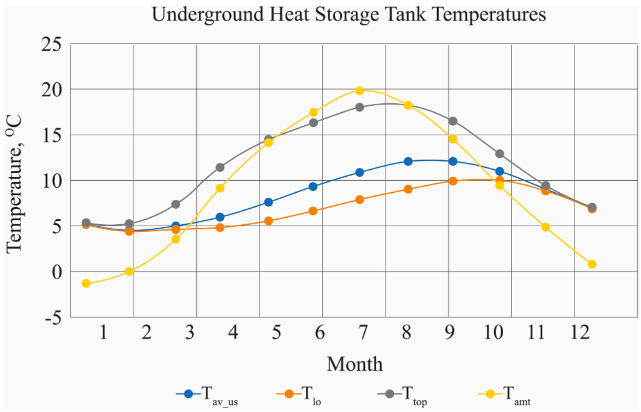

Fig. 21. Underground thermal energy storage unit temperature.

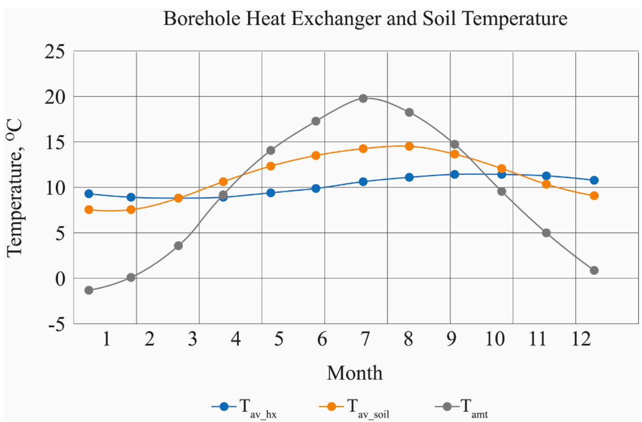

Fig. 22. Borehole heat exchanger and soil temperature.

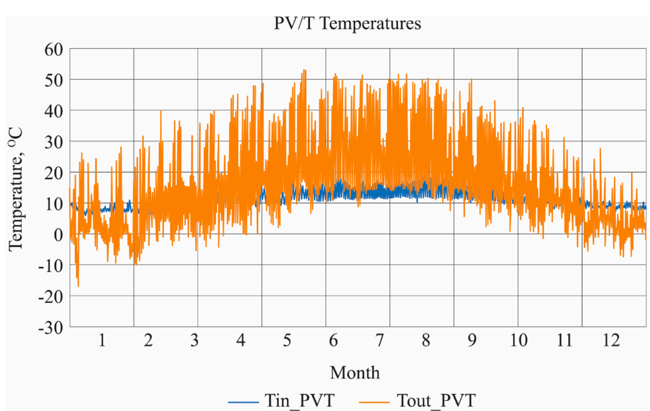

Fig. 23. PV/T system temperatures.

the CH buffer tank. When the temperature in the DHW tank drops, the DHW water circulates through the heat exchanger of the CH buffer tank.

The connections between the heat pump, underground heat storage tank, and borehole heat exchanger, along with pumps, bypass, and diverters, are shown in Fig. 15.

Two sun-tracking PV/T systems, each consisting of 12 PV/T panels, are modeled as illustrated in Fig. 16. The waste heat from the PV/T systems is used to regenerate borehole heat exchangers. When the outlet temperature of the sun-tracking solar collectors is low, the thermal energy is used to store in the underground thermal energy storage unit.

5. Results and discussion

In this section, the simulation results, including monthly thermal energy and electricity generation and consumption, heat pump energy profile, the temperature profile of solar collectors, borehole heat exchanger, underground heat storage tank, and PV/T system, are presented. The summary of energy analysis is given in Table 11.

The general energy demand and generation, including thermal energy generation, electricity generation, and consumption, are shown in Fig. 17. In Fig. 17, Q_{total} is the total energy demand of the storey, including CH, DHW, and losses. Q_{hp}, Q_{solar}, and Q_{pvt} are the thermal energy generation of heat pump, solar collectors, and PV/T system, respectively. P_{hp} is the electricity consumption of the heat pump. $P_{pv\text{-}pvt}$ indicates the total electricity generation of the PV and PV/T systems.

Simulation results show that the HP consumes 9.02 MWh/y of electricity during the yearly working period, and the electricity consumption of the control system, pumps, and system losses are around 4.22 MWh/y. The total electricity consumption of the RESHeat system is 13.24 MWh/y for this demo site. The yearly electricity generation of PV and PV/T systems are 17.89 MWh/y and 11.74 MWh/y, respectively. Monthly electricity generation and consumption are shown in Fig. 18. During the summer, the PV and PV/T systems' electricity production can cover the RESHeat system's electricity consumption. The excess electricity is stored in the grid to be used during the heating season.

The yearly solar collector thermal energy generation is 22.65 MWh/y. The monthly storey central heating and domestic hot water demand, along with solar collector energy generation, is given in Fig. 19. The yearly thermal energy generated by sun-tracking solar collectors is able to cover 46 % of the heating demand of the building.

In Fig. 19, Q_{solar} and Q_{pvt} represent the thermal energy generated by solar collectors and PV/T systems, whereas Q_{ch} and Q_{dhw} stand for the thermal energy demand for central heating and domestic hot water preparation. The heat pump heat generation and monthly total thermal energy demand, including central heating demand, domestic hot water demand, and losses, are shown in Fig. 20. In Fig. 20, Q_{hp} indicates the thermal energy generated by the heat pump, and Q_{total} is the total thermal energy demand of the storey, monthly.

During the heating season, the thermal energy generation of sun-tracking solar collectors and PV/T systems is low, and the heat pump actively works to cover the demand.

The temperature variation in the underground heat storage tank is presented in Fig. 21. T_{top} and T_{lo} stand for the top side temperature of the underground storage tank and the bottom side temperature of the underground storage tank. T_{av_us} and T_{amt} are the mean temperatures of the tank and ambient temperature over the year. During the non-heating season, the waste heat is stored in the underground thermal energy storage unit to be used during the heating season.

Fig. 22 illustrates the temperature variation in the borehole heat exchanger and the soil temperature around it. T_{av_hx} and T_{av_soil} stand for the average borehole heat exchanger temperature and soil temperature, respectively.

The variation of temperature in the inlet and outlet of the PV/T system is given in Fig. 23. T_{in_PVT} is the temperature variation in inlet temperature over the year. T_{out_PVT} is the outlet temperature of the PV/T system during the year.

In Fig. 24, the monthly average COP trend of the heat pump is illustrated. The simulations show that the yearly average COP of the heat pump is 4.85. The COP of the heat pump is kept over 4.50 during a year-round simulation thanks to the thermal energy stored in the underground thermal energy storage unit and the borehole heat exchangers.

6. Conclusions

In this paper, integration of the experimentally validated RESHeat system components for a residential building is carried out using TRNSYS software. The demo site building model is developed to study

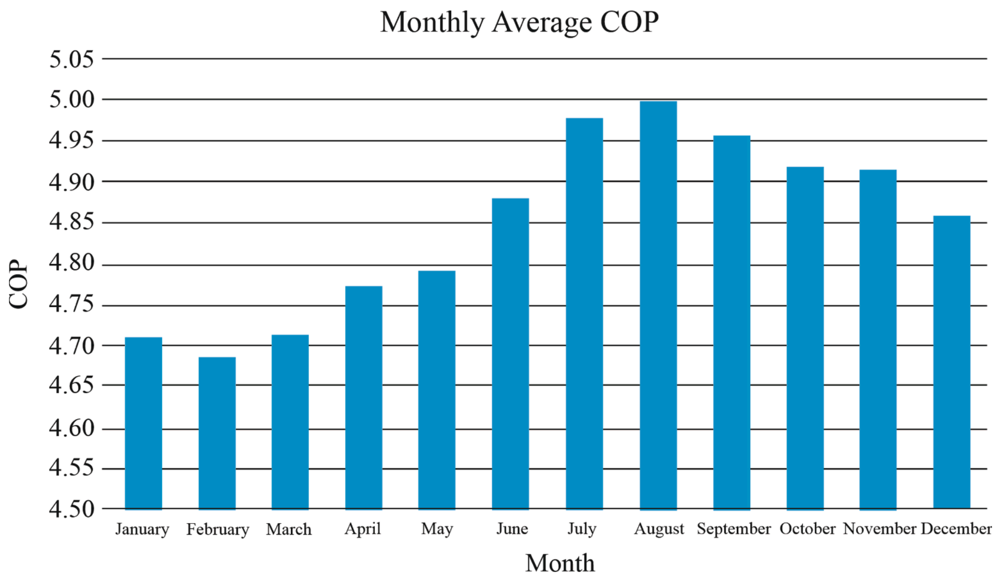

Fig. 24. Monthly average COP trend of the heat pump.

energy demand, and then the RESHeat system is implemented. The transient behavior of the system is analyzed. The results show that the RESHeat energy system is applicable for residential buildings to cover central heating, domestic hot water and electricity demand. Several significant findings have resulted from this study and are summarized as follows:

- The total central heating and domestic hot water demands, including losses, are found to be 52.80 MWh/y for the storey of the building.
- The heat pump's thermal energy generation is 42.19 MWh/y, whereas the electricity consumption of the heat pump is 9.02 MWh/y.
- The thermal energy produced by PV/T systems and sun-tracking solar collectors is 14.19 and 22.65 MWh/y, respectively.
- The electricity generated by PV modules and PV/T systems is 17.89 and 14.19 MWh/y.
- The yearly average COP of the heat pump is 4.85.
- The energy consumption coverage of the RESHeat system for the storey of the demo site is 100 %.
- The average error between the model and experimental data is 0.22 %, 3.77 %, 4.74 %, and 0.98 % for the PV module, sun-tracking solar collector, sun-tracking PV/T system, and underground storage unit, respectively.
- The heat pump's COP, heating capacity, electricity consumption data, and model error are 0.44 %, 0.22 %, and 0.34 %, respectively.

The RESHeat system is also implemented in a residential building located in Palombara Sabina, Italy. The primary purpose of the system implementation in Italy is to test the RESHeat system integration with building in different climates. The building heating and cooling demands are 54.92 and 37.70 MWh/y, respectively. The RESHeat system contains a stationary PV/T system, heat storage tanks, a dry cooler, a heat pump, and fan coils. The water-to-water heat pump generates thermal energy for winter heating and summer cooling. The PV/T system is coupled with a heat storage tank on the source side of the heat pump. The load side of the heat pump is connected to fan coils for cooling and space heating. The storage tank is also connected to the dry cooler to remove heat during the summer season.

The major importance of RESHeat solution is ground heat source regeneration through PVT waste heat, which allows for achieving a high COP value of the heat pump. Therefore the compressor is not overloaded. Therefore, RESHeat solution benefits from long-term heat pump usage at high efficiency. The high COP value in consecutive years is fundamental for long-term prediction of the economic benefits of heat-pump heating/cooling systems. The RESHeat system allows the creation of a modern, competitive, and climate-neutral energy system to help Europe's commitment to lead in global climate action and lead to achieving net-zero greenhouse gas emissions. The proposed system can help with energy transition in the EU tremendously as the system can be retrofitted to residential buildings to cover energy demand.

The RESHeat system is currently integrated at three demo sites. Two demo sites are located in Poland, and the last one is in Italy. Once the RESHeat system integration with residential buildings is completed, energy efficiency measurements will be conducted, including electrical energy, thermal energy, room temperatures, COP value, the energy usage of the heat pump, and thermal comfort. The actual data will then be compared to the simulation results obtained for the demo site in Limanowa, Poland. In addition, an economic analysis of the cost-effectiveness of the RESHeat system is planned to be performed using the net present value (NPV) method.

CRediT authorship contribution statement

Mehmet Ali Yildirim: Software, Validation, Writing - original draft. **Filip Bartyzel:** Methodology, Conceptualization. **Andrea Vallati:** Methodology, Conceptualization. **Magdalena Kozień Woźniak:** Formal analysis, Writing – review & editing. **Paweł Ocłoń:** Writing – review & editing, Funding acquisition, Project administration.

Declaration of Competing Interest

The authors declare that they have no known competing financial interests or personal relationships that could have appeared to influence the work reported in this paper.

Data availability

No data was used for the research described in the article.

Acknowledgements

The research was supported by European Commission and is a part of the HORIZON 2020 project RESHeat. This project received funding from the Horizon 2020 framework program in theprogram in the field of research and innovation on the basis of grant agreement No. 956255. This research was supported by Center for Scientific Research Excellence of Cracow University of Technology and performed within a multidisciplinary group: Storage and Transmission of Electricity and Heat.

References

[1] Parliament, Council of the European Union. Directive 2010/31/EU of the European Parliament and of the Council of 19 May 2010 on the energy performance of buildings (recast), 2010. http://data.europa.eu/eli/dir/2010/31/oj.

[2] Commission Recommendation (EU) 2016/1318 of 29 July 2016 on guidelines for the promotion of nearly zero-energy buildings and best practices to ensure that, by 2020, all new buildings are nearly zero-energy buildings. Official J. 2016;46–57. http://data.europa.eu/eli/reco/2016/1318/oj.

[3] Regulation of the Ministry of Infrastructure of 12 April 2002 on the technical conditions which should be met by buildings and their location, Annex to the notice. Technical conditions to be met by buildings and their location, Annex to the Announcement Minister of Development and Technology of 15 April 2022, Dz.U. 2022 item 1225. (in Polish).

[4] A long-term strategy for building renovation. Supporting the renovation of the national building stock. Annex to Resolution No. 23/2022 of the Council of Ministers of 9 February 2022. https://zae.org.pl/wpcontent/uploads/2022/02/Dlugoterminowa_strategia_renowacji_budynkow_gov.pdf, (in Polish).

[5] Directive (Eu) 2018/844 of the European Parliament and of the Council of 30 May 2018 amending Directive 2010/31/EU on the energy performance of buildings and Directive 2012/27/EU on energy efficiency, 2018. http://data.europa.eu/eli/dir/2018/844/oj.

[6] Rabani M, Madessa HB, Nord N. Achieving zero-energy building performance with thermal and visual comfort enhancement through optimization of fenestration, envelope, shading device, and energy supply system. Sustain Energy Technol Assess 2021;44. https://doi.org/10.1016/j.seta.2021.101020.

[7] Hong Y, Ezeh CI, Deng W, Hong S-H, Ma Y, Tang Y, et al. Coordinated energy-environmental-economic optimization of building retrofits for optimal energy performance on a macro-scale: A life-cycle cost-based evaluation. Energ Conver Manage 2021;243. https://doi.org/10.1016/j.enconman.2021.114327.

[8] Wang Z, Liu X, Deng G, Shen H, Xu Z. A framework for retrofitting existing houses to nearly zero energy buildings: Development and a real-life case study. Energ Build 2021;252. https://doi.org/10.1016/j.enbuild.2021.111438.

[9] Fina B, Auer H, Friedl W. Profitability of active retrofitting of multi-apartment buildings: Building-attached/integrated photovoltaics with special consideration of different heating systems. Energ Build 2019;190. https://doi.org/10.1016/j.enbuild.2019.02.034.

[10] Rafał B, Jakub B, Agnieszka C, Rita Ł, Renata P. Renewable Energy Sources vs. an Air Quality Improvement in Urbanized Areas - the Metropolitan Area of Kraków Case. Front Energy Res 2021;9. https://doi.org/10.3389/fenrg.2021.767418.

[11] Godin K, Sapinski JP, Dupuis S. The transition to net zero energy (NZE) housing: An integrated approach to market, state, and other barriers. Clean Respons Consum 2021;3. https://doi.org/10.1016/j.clrc.2021.100043.

[12] Mazzeo D, Matera N, Cornaro C, Oliveti G, Romagnoni P, Santoli LD. EnergyPlus, IDA ICE and TRNSYS predictive simulation accuracy for building thermal behaviour evaluation by using an experimental campaign in solar test boxes with and without a PCM module. Energ Build 2020;212. https://doi.org/10.1016/j.enbuild.2020.109812.

[13] Quesada B, Sánchez C, Cañada J, Royo R, Payá J. Experimental results and simulation with TRNSYS of a 7.2kWp grid-connected photovoltaic system. Appl Energy 2011;88:1772–83. https://doi.org/10.1016/j.apenergy.2010.12.011.

[14] Kenai MA, Libessart L, Lassue S, Defer D. Impact of green walls occultation on energy balance: Development of a TRNSYS model on a brick masonry house. J Build Eng 2021;44. https://doi.org/10.1016/j.jobe.2021.102634.

[15] Bordignon S, Emmi G, Zarrella A, Carli MD. Energy analysis of different configurations for a reversible ground source heat pump using a new flexible TRNSYS Type. Appl Therm Eng 2021;197. https://doi.org/10.1016/j.applthermaleng.2021.117413.

[16] Eddib F, Lamrani MA, Bouyahia SA. TRNSYS validation of a study on building's energetic evaluation in North of Morocco. Energy Procedia 2017;139:334–9. https://doi.org/10.1016/j.egypro.2017.11.217.

[17] Potočnik P, Vidrih B, Kitanovski A, Govekar E. Analysis and optimization of thermal comfort in residential buildings by means of a weather-controlled air-to-water heat pump. Build Environ 2018;140:68–79. https://doi.org/10.1016/j.buildenv.2018.05.044.

[18] Mansir IB, Hani EHB, Farouk N, AlArjani A, Ayed H, Nguyen DD. Comparative transient simulation of a renewable energy system with hydrogen and battery energy storage for residential applications. Int J Hydrogen Energy 2022;47: 26198–208. https://doi.org/10.1016/j.ijhydene.2022.02.092.

[19] Belmonte JF, Díaz-Heras M, Almendros-Ibáñez JA, Cabeza LF. Simulated performance of a solar-assisted heat pump system including a phase-change storage tank for residential heating applications: A case study in Madrid, Spain. J Storage Mater 2022;47. https://doi.org/10.1016/j.est.2021.103615.

[20] Yuan X, Heikari L, Hirvonen J, Liang Y, Virtanen M, Kosonen R, et al. System modelling and optimization of a low temperature local hybrid energy system based on solar energy for a residential district. Energ Conver Manage 2022;267. https://doi.org/10.1016/j.enconman.2022.115918.

[21] Endo N, Shimoda E, Goshome K, Yamane T, Nozu Ti, Maeda T. Simulation of design and operation of hydrogen energy utilization system for a zero emission building. Int J Hydrogen Energy 2019;44. https://doi.org/10.1016/j.ijhydene.2019.01.232.

[22] Rashad M, Żabnieńska-Góra A, Norman L, Jouhara H. Analysis of energy demand in a residential building using TRNSYS. Energy 2022;254. https://doi.org/10.1016/j.energy.2022.124357.

[23] Hernández-Arizaga A, Picallo-Pérez A, Sala-Lizarraga JM. Procedure for modelling and calibrating operating thermal systems in buildings. J Build Eng 2022;45. https://doi.org/10.1016/j.jobe.2021.103530.

[24] Baldinelli G, Schnotale JA, Bianchi F, Lechowska AA, Presciutti A. An environment-adaptive wall: concept, implementation and effects on the energy performance of a residential building. Energ Build 2022;68. https://doi.org/10.1016/j.enbuild.2022.112209.

[25] Lin Y, Feng H, Yang W, Hao X, Tian L, Yuan X. Thermal performance optimization of a semi-nested building coupled with an earth-to-air heat exchanger using iterative Taguchi method. Renew Energy 2022;195:1275–90. https://doi.org/10.1016/j.renene.2022.06.116.

[26] Açıkkalp E, Caliskan H, Hong H, Piao H, Seung D. Extended exergy analysis of a photovoltaic-thermal (PVT) module based desiccant air cooling system for buildings. Appl Energy 2022;323. https://doi.org/10.1016/j.apenergy.2022.119581.

[27] Mehmood S, Lizana J, Núñez-Peiró M, Maximov SA, Friedrich D. Resilient cooling pathway for extremely hot climates in southern Asia. Appl Energy 2022;325. https://doi.org/10.1016/j.apenergy.2022.119811.

[28] Naji S, Aye L, Noguchi M. Sensitivity analysis on energy performance, thermal and visual discomfort of a prefabricated house in six climate zones in Australia. Appl Energy 2021;298. https://doi.org/10.1016/j.apenergy.2021.117200.

[29] Sakellariou EI, Axaopoulos PJ. Energy performance indexes for solar assisted ground source heat pump systems with photovoltaic-thermal collectors. Appl Energy 2020;272. https://doi.org/10.1016/j.apenergy.2020.115241.

[30] Kavian S, Aghanajafi C, Mosleh HJ, Nazari Ar, Nazari As. Exergy, economic and environmental evaluation of an optimized hybrid photovoltaic-geothermal heat pump system. Appl Energy 2020;276. https://doi.org/10.1016/j.apenergy.2020.115469.

[31] Rohde D, Andresen T, Nord N. Analysis of an integrated heating and cooling system for a building complex with focus on long–term thermal storage. Appl Therm Eng 2018;145. https://doi.org/10.1016/j.applthermaleng.2018.09.044.

[32] Ozyogurtcu G, Mobedi M, Ozerdem B. Economical assessment of different HVAC systems for an operating room: Case study for different Turkish climate regions. Energy Build 2011;43. https://doi.org/10.1016/j.enbuild.2011.02.013.

[33] CIBSTE. Guide B1: heating. 2016.